

## ESTIMATION OF MOLECULAR MOBILITY OF AMORPHOUS DISACCHARIDES

Mikaela Hautaniemi  
University of Helsinki  
Faculty of Pharmacy  
Division of Pharmaceutical Technology  
Industrial Pharmacy

May 2012

Tiedekunta – Fakultet – Faculty Farmasian tiedekunta		Osasto – Sektion – Department Farmasian teknologian osasto	
Tekijä – Författare – Author Mikaela Hautaniemi			
Työn nimi – Arbetets titel – Title Amorfisten disakkaridien molekylaarisen mobilitettiin tutkiminen			
Oppiaine – Läroämne – Subject Teollisuusfarmasia			
Työn laji – Arbetets art – Level Pro gradu -tutkielma		Aika – Datum – Month and year Toukokuu 2012	Sivumäärä – Sidoantal – Number of pages 53
<p> Tiivistelmä – Referat – Abstract  Lääkevalmistuksessa amorfista muotoa käytetään, esimerkiksi parantamaan liukoisuusnopeutta, stabiloimaan proteiinien rakennetta säilytyksen aikana ja parantamaan apuaineiden käsiteltävyyttä. Aine voi muuttua osittain tai kokonaan amorfiseen muotoon monen tavallisen lääkevalmistusprosessin, kuten kalvopäällystyksen, rakeistuksen, kuivauksen, jauhatuksen ja puristuksen seurauksena. Amorfisten alueiden läsnä ollessa aineen fysikaaliset ominaisuudet muuttuvat merkittävästi, mikä vaikuttaa lääkevalmisteen fysikaaliseen ja kemialliseen säilyvyyteen. </p> <p> Amorfisen aineen molekyylimobilitaetti on tärkeä lasitilan pysyvyyttä kuvaava parametri. Tämän vuoksi on tärkeää arvioida se lääkekoostumussuunnittelun alkuvaiheessa. </p> <p> Tutkimuksen tavoitteena oli määrittää differentiaalista pyyhkäisykalorimetriaa (<i>DSC</i>) apuna käyttäen neljän amorfisen disakkaridin molekyylimobilitaettia alhaisissa (verrattuna <math>T_g</math>:seen) lämpötiloissa. Relaksaatio tapahtuu tutkituissa lämpötiloissa hyvin hitaasti. Niin hitaasti, että alkurelaksaationopeutta voidaan käyttää hyväksi relaksaatioprosessin kokonaisuuden arvioinnissa. </p> <p> Tutkimuksessa käytetyillä disakkarideilla on todettu olevan samanlainen relaksaatiotaipumus, kun tätä arvioidaan lasisiirtymälämpötilan (<math>T_g</math>) -arvon perusteella. Korkeamman <math>T_g</math>:n omaavilla yhdisteillä lasitila on tavallisesti pysyvämpi. Sakkaroosin <math>T_g</math> on alhaisin tutkimuksessa käytetyistä disakkarideista. Amorfisella mellibioosilla, trehaloosilla ja selibioosilla on kahden vuoden relaksaatioaika säilytettäessä lämpötilassa <math>T_g-55^{\circ}\text{C}</math>. Amorfisen sakkaroosin kohdalla tarvitaan alhaisempi säilytyslämpötila (<math>T_g-70^{\circ}\text{C}</math>) samansuuruisen relaksaationopeuden saavuttamiseen. </p> <p> Fragiliteettia voidaan käyttää amorfisten aineiden luokitteluun ja vertailuun. Kaikki tutkimuksessa käytetyt disakkaridit voidaan luokitella hauraksi yhdisteiksi. Fragiliteetin arvot laskettiin kolmen eri menetelmän avulla. Tuloksina saatiin kolme jossain määrin erilaista fragiliteettijärjestystä. Tulosten epäytenevyys johtuu ainakin osittain <i>DSC</i> -laitteiston ominaisuuksista. Tutkimuksessa käytettyä menetelmää on vaikea soveltaa ilman muiden menetelmien tukitietoja. <math>T_g</math>:n riippuvuudella lämmitysnopeudesta on tärkeä merkitys, tästä syystä pienikin poikkeama ko. arvoissa saa aikaan merkittävät muutokset lopputulokseen. Tästä huolimatta tutkimuksen lopputuloksena saatujen relaksaatioajan arvojen voidaan todeta olevan yhdenmukaisia aikaisimpien tutkimuksien kanssa. </p>			
Avainsanat – Nyckelord – Keywords amorfinen, differentiaalinen pyyhkäisykalorimetria ( <i>DSC</i> ), relaksaatioaika, kylmäkuivaus			
Säilytyspaikka – Förvaringställe – Where deposited Farmasian Teknologian osasto, Helsingin Yliopisto			
Muita tietoja – Övriga uppgifter – Additional information Ohjaaja: Petteri Heljo (tutkija, HY)			

HELSINGIN YLIOPISTO – HELSINGFORS UNIVERSITET – UNIVERSITY OF HELSINKI

Tiedekunta – Fakultet – Faculty Faculty of Pharmacy		Osasto – Sektion – Department Division of Pharmaceutical Technology	
Tekijä – Författare – Author Mikaela Hautaniemi			
Työn nimi – Arbetets titel – Title Estimation of molecular mobility of disaccharides			
Oppiaine – Läroämne – Subject Industrial Pharmacy			
Työn laji – Arbetets art – Level Master thesis		Aika – Datum – Month and year May 2012	Sivumäärä – Sidoantal – Number of pages 53
<p>Tiivistelmä – Referat – Abstract</p> <p>In pharmaceuticals amorphous state can be obtained either intentionally or unintentionally. Intentional production is used, for example, to improve the dissolution of poorly soluble compounds, to stabilize the structure of proteins, or to improve the mechanical properties of excipients (e.g., lactose). Unintentional introduction of amorphous phases can result from general manufacturing procedures of pharmaceuticals, such as coating, granulation, drying, milling, and compression. The presence of amorphous regions, even in small quantities, can exhibit a significant influence on the physical and chemical stability of pharmaceutical products.</p> <p>Molecular mobility in formulation with amorphous content is believed to be the key factor of their stability. Therefore, evaluating of molecular mobility is an important step in pharmaceutical product development.</p> <p>The aim of this study was to estimate molecular motions in amorphous disaccharides using calorimetric approach at temperatures below the glass transition temperature (<math>T_g</math>), where relaxation process is very slow as compared to the time of experiment. When temperature is low enough, the initial relaxation time parameter (<math>\tau_i</math>) can be used as an estimate for relaxation process on the timescale of pharmaceutical product shelf life.</p> <p>The results of the present study revealed similar trend in stability of amorphous forms for the disaccharides (sucrose experiencing the fastest structural relaxation), which can be assumed on the basis of <math>T_g</math> alone, where higher <math>T_g</math> would result in more stable glassy state (<math>T_g</math> of sucrose is the lowest). Storage temperature of <math>T_g - 55^\circ\text{C}</math> or lower would suffice for amorphous trehalose, melibiose and cellobiose to achieve at least 2 year's relaxation time, while for sucrose the temperature is <math>T_g - 70^\circ\text{C}</math>.</p> <p>Fragility has been used as a helpful mean for classifying amorphous materials. All the compounds can be classified as fragile. Fragility ranking in the present study contains some degree of uncertainty, while 3 different approaches revealed somewhat different results for ranking the disaccharides. The variation in the results can be attributed to the overall sensitivity of DSC. The method described in the present study is quite difficult to apply without supportive information from other techniques. The results, obtained with the method, are very dependent on the slope in plotting <math>\ln q</math> vs. <math>1/T_g</math>, and even small fluctuations in the estimation can lead to different fragility values and consequently to different relaxation times. However, the final results reveal values for relaxation times well below <math>T_g</math>, which are in reasonable agreement with modern theoretical understanding of glassy state dynamics.</p>			
Avainsanat – Nyckelord – Keywords amorphous, DSC, relaxation time, freeze-drying			
Säilytyspaikka – Förvaringställe – Where deposited Division of Pharmaceutical Technology, Helsingin University			
Muita tietoja – Övriga uppgifter – <input type="checkbox"/> Additional information Instructor: Petteri Heljo (researcher, University of Helsinki)			

## CONTENTS

I	LITERATURE REVIEW .....	1
1	INTRODUCTION.....	1
2	THEORY ASPECTS OF GLASSY STATE.....	3
2.1	Kinetic perspective.....	3
2.2	Changes in enthalpy below the melting point.....	5
2.3	Relaxation phenomena and enthalpy recovery .....	7
2.4	Evaluation of molecular mobility.....	9
2.4.1	Average relaxation time.....	9
2.4.2	Relaxation time at a given temperature.....	11
2.5	Fragility.....	12
3	METHODS OF PRODUCTION OF AMORPHOUS MATERIAL.....	13
3.1	Routes of production of amorphous material in pharmaceuticals.....	13
3.2	Freeze-drying.....	14
3.2.1	Freezing step.....	15
3.2.2	Primary drying.....	18
3.2.3	Secondary drying.....	19
4	METHODS OF CHARACTERIZATION OF AMORPHOUS MATERIAL.....	20
4.1	Diffraction techniques.....	21
4.2	Spectroscopic techniques.....	21
4.3	Dynamic vapour sorption.....	23
4.4	Dielectric relaxation measurements.....	23
4.5	Thermal techniques.....	24
4.5.1	Thermomechanical analysis and dynamic mechanical analysis.....	24
4.5.2	Differential scanning calorimetry.....	26
4.5.3	Modulated differential scanning calorimetry.....	28
4.5.4	Isothermal microcalorimetry.....	30
II	EXPERIMENTAL PART.....	31
5	THE AIM OF THE STUDY.....	31
6	METHOD DEVELOPMENT.....	32
7	MATERIALS AND METHODS.....	34
8	RESULTS AND DISCUSSION.....	37
8.1	The heat capacity measurements and $\gamma$ -parameter.....	37
8.2	Fragility.....	40
8.3	Initial relaxation time.....	43
8.4	Other stability considerations for formulation with amorphous content.....	45
9	CONCLUSIONS.....	46
10	REFERENCES.....	48

## LIST OF ABBREVIATIONS

$C_p$	heat capacity
D	strength parameter
DSC	differential scanning calorimetry
$E_a$	activation energy
H	enthalpy
IR	infrared
KWW	Kohlrausch-Williams-Watts (equation)
m	steepness index
NMR	nuclear magnetic resonance
q	heating rate
RH	relative humidity
S	entropy
$S_c(T)$	configurational entropy at temperature T
T	temperature
t	time
$T_f$	fictive temperature
$T_g$	glass transition temperature
$T_g'$	glass transition temperature of a mixture of 2 or more compounds
TK	Kauzman temperature
$T_m$	melting point
$V_{free}$	free volume
VTF	Vogel-Tamman-Fulcher
$\beta$ or $\beta_{KWW}$	distribution parameter
$\tau$	relaxation time
$\tau_0$	relaxation time constant, ( $10^{-14}$ s)

## I LITERATURE REVIEW

### 1 INTRODUCTION

Successful drug development results in a reliable product with consistent performance. Formulations with amorphous content have got much attention within pharmaceutical industry due to their properties that differ significantly from those of crystalline material.

Below the melting point a liquid can crystallize, forming thermodynamically stable structure. In this case molecules arrangement has a certain pattern, typical for the material. However, it does not always happen this way. For example, rapid cooling below melting point can result in rubbery state, and as temperature is reduced further, an amorphous or glassy state can be formed. Kinetically, a glass structure brings in mind a structure of a liquid, where molecules do not have long range order. In terms of thermodynamics a glass possesses higher enthalpy than corresponding crystalline form. These properties inevitably generate stability issues related to amorphous state, since loosely packed structure of a glass tends to relax with time towards an equilibrium, as material experiences structural and orientational changes.

The relevance of amorphous state to pharmaceuticals can be explained by its common occurrence. Standard pharmaceutical procedures, such as coating, granulation, drying, milling, and compression can result in solids, which are completely or partially amorphous. The presence of amorphous regions, even in small quantities, can exhibit a significant influence on the physical and chemical stability of pharmaceutical products (Hancock and Zografi 1997).

In many cases amorphous state is obtained deliberately. Intentional production is used, for example, to improve the dissolution of poorly soluble compounds (Law et al. 2001), to stabilize the structure of proteins (Carpenter et al. 1997), or to improve the mechanical properties of excipients. For some pharmaceutical formulations freeze-drying or lyophilisation is the technique of choice. It allows to stabilize heat and water labile substances and improve bioavailability of poorly soluble drugs.

Choice of excipients is crucial for lyophilized formulation. A considerable number of research articles exists, where different excipients for formulations with amorphous content are compared (Constantino et al. 1998; Mazzobre et al. 2001; Liao et al. 2002; Chang et al. 2005; Wang et al. 2009).

Many carbohydrates have been reported to be found in significant amount in various organisms, which are able to survive severe dehydration (Crowe 1998). One of the theories explains the mechanism of life preservation to be based on the ability of carbohydrates to form a glass and support the cell organs, when water is removed from the system. There are differences in the intrinsic properties of different amorphous solids, which cannot always be attributed to the molecular weight of the carbohydrates alone, but must arise from other characteristics of carbohydrates. Due to high viscosity and specific interactions (hydrogen bonding) with protein structures, the glassy matrix is assumed to reduce any motions of labile molecules (Allison et al. 1996). The purpose of the study is to get an insight to the ability of the molecules for biopreservation, the principle, which has been applied in pharmaceuticals for protection of labile substances (such as proteins) during freeze-drying (Wang 2000) and storage for the time of amorphous drug products desired shelf life.

It is generally accepted, that the stability issues, related to amorphous material, arise from greater molecular mobility as compared to crystalline form. The aim of this study is to estimate molecular motions in structurally related amorphous disaccharides using calorimetric approach at temperatures below  $T_g$ , where relaxation process is very slow as compared to the time of experiment. When temperature is low enough, changes in molecular mobility occur very slowly as well. In this case the relaxation time parameter of a glass, thermal history of which has been erased, could be used as an estimate for relaxation process on the timescale of pharmaceutical product shelf life. The technique, if valid, would provide a fast, low sample requirement and widespread instrumentation method, which can be especially helpful in preformulation.

## 2. THEORY ASPECTS OF GLASSY STATE

### 2.1 Kinetic perspective

There are three traditional states of matter or phases: solid, liquid and gas. A transfer from one state of matter to another usually involves a release or absorption of heat. In solids and liquids, neighbour molecules' forces of attraction and repulsion contribute to the physical properties the substance.

Let us consider two atoms' system in a crystal. There is some empty space between any two atoms of a solid. That is because the atoms do not only attract but also push each other away. The negatively charged electron clouds govern to a large extend the balance of forces between two atoms. The repulsion increases exponentially with a decrease in distance between the molecules. An equilibrium distance  $r_0$ , about  $(3 \text{ to } 4) \times 10^{-8} \text{ cm}$  (3-4 angstroms) is the distance between two atoms where the forces of attraction and repulsion are balanced (see Figure 1). In this position one atom's potential energy in the other atom's electric field is minimized. The atom's position change would need some work to overcome the atoms' attractive and distractive forces.

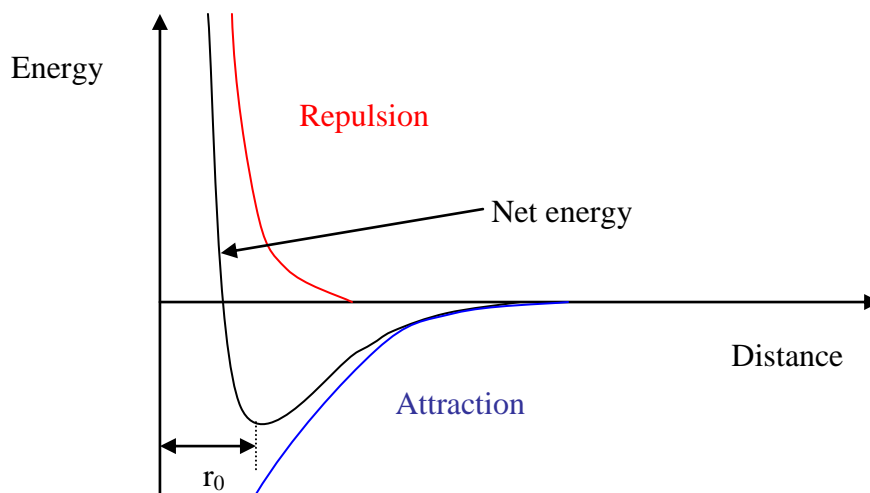


Figure 1. Repulsive and attractive energies and net energy as function of the distance between atoms. At equilibrium distance,  $r_0$ , the repulsive and attractive forces between molecules are equal.

When some heat is supplied to a substance in a solid state that means the atoms' kinetic energy increases. The changes in kinetic and potential energy are balanced through atom's



electric fields. The atom is said to oscillate about the potential energy minima. So, when some heat is supplied to the substance, the substance expands.

When atom's kinetic energy increases sufficiently, the atom can move from one neighbour's electric field to another. A solid turns into a liquid, which shape can change with the shape of its container. When atoms get enough energy, they can overcome neighbour's attraction forces. The substance becomes a gas.

So, a solid is formed when the atom's or molecules kinetic energy decreases to the extent that they cannot overcome neighbours attraction forces. When the system is cooled slowly, atoms can form regular lattice, with repeating order, which is typical for the substance. The structure usually provides a minimum of potential energy and maximum amount of bonds to the neighbour atoms, which stabilizes the system.

A liquid can be cooled so rapidly that there is no time to form a lattice. In this case below the melting point a supercooled liquid is formed. In this state the immediate bunch (group) of neighbours for a molecule remains the same for a measurable period of time, reaching 100s at  $T_g$  (compared to the liquid state, where any two molecules are reluctant to stay together for any meaningful period of time). As the temperature is reduced further, at the glass transition temperature an amorphous state is entered. The substance behaves solid-like, but molecules lack of order brings in mind the structure of a liquid just before the moment of freezing. Molecules are not in their most stable position of neighbours' electric field. Their position in the neighbour's network is said to be frozen and the system is said to be kinetically trapped. At this point molecules do not possess enough energy to form an ordered structure during the time of observation. Potential energy barriers are large compared to thermal energy of the molecules, when the material is in glassy state (Goldstein 1969). A kinetic barrier to crystallization can be defined as free energy of activation for the short-range dislocation/moving of molecules to enter a lattice position. Each frozen liquid has its own structure and mode of structural rearrangement (Moynihan 1995).

The bonds between atoms or molecules determine the physical properties of a substance. Primary packing rule for crystal structure is the drive to maximize density and minimize free volume (Tang et al. 2002). In some of the crystal structures the opportunity to maximize the hydrogen bonding interactions has been sacrificed for other packing factors. Hydrogen bond

intensity for some substances in amorphous state can be more comprehensive than in the crystalline. For example, for felodipine hydrogen bonding in crystalline state is weaker than in amorphous, so the last form is more stable than amorphous forms of other, structurally related materials (Marsac et al 2006).

## 2.2 Changes in enthalpy below the melting point

Rapid cooling of a liquid below melting point creates the kinetic considerations discussed above. Aside from it, there are also explicit thermodynamic changes involved. Figure 2 illustrates key differences in formation of amorphous and crystalline systems.

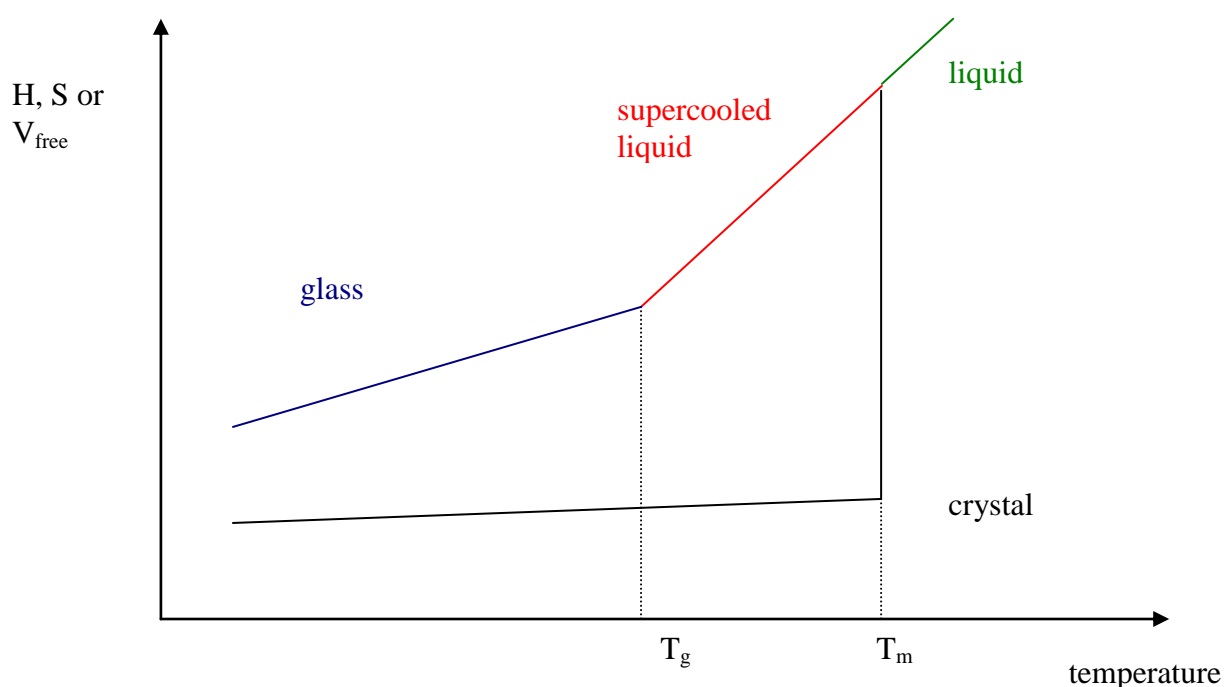


Figure 2. Schematic illustration of the change in volume, enthalpy or entropy with temperature for a material undergoing crystallisation or a glass transition.  $T_m$  is the melting temperature;  $T_g$  is the glass transition temperature.

Below the melting point a liquid can crystallize, forming thus a thermodynamically stable structure. Crystallisation is an exothermic process accompanied by a rapid free volume loss. Thus, both the enthalpy (H) and specific volume (V) decrease can be defined at melting point during crystallization. As the temperature is reduced further, the above mentioned properties decrease as well, but the change is less noticeable. It should be mentioned; however, that one of the water anomalies is that crystallisation is rather followed by an expansion than a contraction of the system.

On the other hand, when a liquid is cooled rapidly, there is no time for an ordered structure to be formed. In this case below the melting point a supercooled liquid or rubbery state is entered. No abrupt change in enthalpy or volume follows. On further cooling a point is reached, when the material develops solid-like properties. The structure gets ‘frozen’ into the glassy state. At this point enthalpy trend changes its direction to become less dependent on the temperature. It is still decreasing with temperature, but the decrease is less pronounced with respect to temperature change. That could be the way for the nature to avoid “Kauzmann paradox”. In his famous paper Kauzman (Kauzman 1948) identified thermodynamic crises for supercooled liquids, when temperature lowering below  $T_k$  would reveal unphysical values of enthalpy or entropy for supercooled liquids (see Figure 3).

At the glassy state formation point a stepwise change in heat capacity decrease can be observed calorimetrically. The change of state is defined as glass transition. The temperature of the event is called glass transition temperature,  $T_g$ .

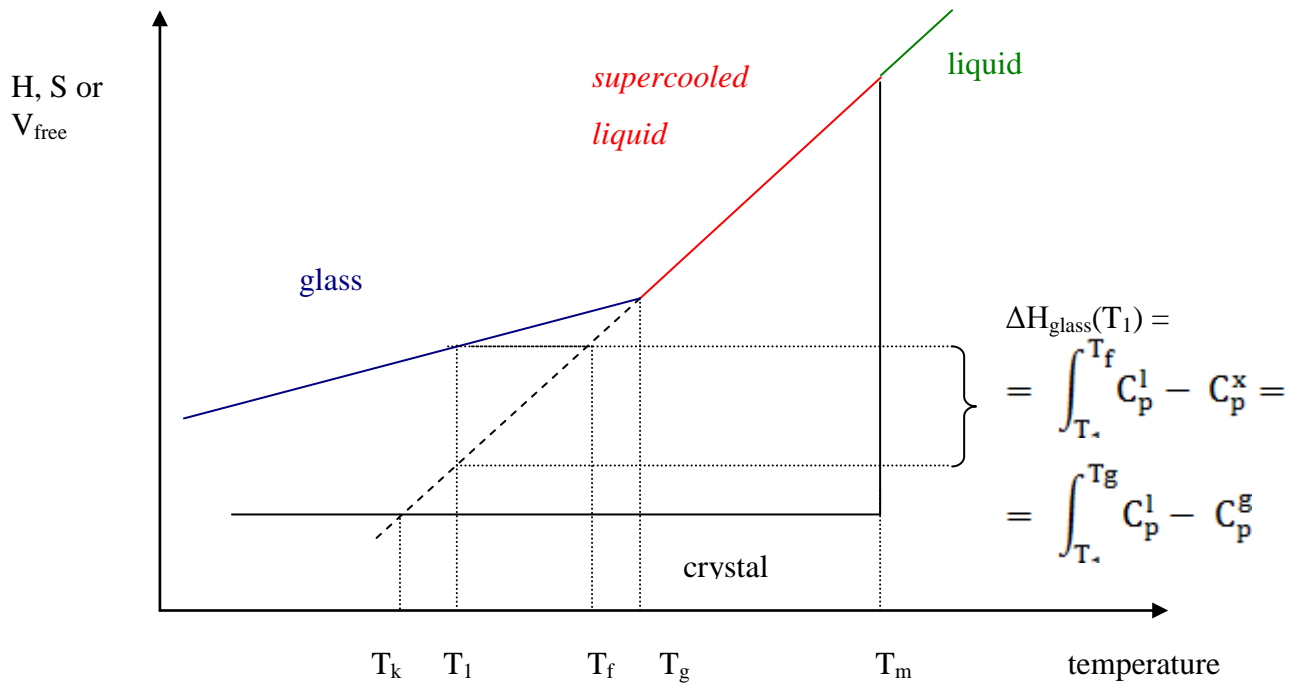


Figure 3. Schematic presentation of fictive temperature and enthalpy of a glass available for relaxation at temperature  $T_1$ . Here  $T_K$  is the temperature at which supercooled liquid's enthalpy is equal to crystal's one. The temperature  $T_k$  is known as Kauzmann temperature.  $C_p^l$  is the heat capacity of liquid form,  $C_p^g$  is the heat capacity of glass,  $C_p^x$  is the heat capacity of crystalline form.

Enthalpy of a glass can be defined in terms of fictive temperature,  $T_f$  (see Figure 3). For this propose, the supercooled liquid's enthalpy line is extrapolated to the glassy state temperatures. Supercooled liquid can show equilibrium behaviour as long as crystallization is hindered. The fictive temperature is the temperature at which the enthalpy of the glass at  $T_1$  is equal to the enthalpy of supercooled liquid at  $T_f$ .

The value of  $T_f$  can be estimated using temperature dependence of heat capacity. The enthalpy available for relaxation  $\Delta H_{\text{glass}}$  of an amorphous material at temperature  $T_1$ , can be defined either in terms of  $T_g$  or  $T_f$ :

$$\begin{aligned} \Delta H_{\text{glass}}(T_1) &= \\ &= \int_{T_g}^{T_f} C_p^l - C_p^x = \int_{T_g}^{T_g} C_p^l - C_p^g \end{aligned} \quad (1)$$

where  $C_p^l$  is the heat capacity of liquid form,  $C_p^g$  is the heat capacity of glass,  $C_p^x$  is the heat capacity of crystalline form.

Fictive temperature method does not demand direct glass transition observation. That is true benefit, while using conventional DSC, when relaxation endotherm superposition may inflect the value of  $C_p$  change at  $T_g$ .

### 2.3 Relaxation phenomena and enthalpy recovery

Constituents of a liquid have translational and reorientational degrees of freedom. There are no fixed positions for the constituents in liquid state. They move in the electric fields of nearest neighbours, using for the movement the energy, which is available at the temperature. During the glass transition the degrees of freedom get frozen out. That means the constituents get frozen to the place and orientation they happened to have at the moment of quenching. A glass is trapped in a single configuration state below  $T_g$ . The structure is not stable, it tends to relax.

Structural relaxation describes changes in glass, when constituents rearrange towards equilibrium of lower energy and higher density. The rearrangement includes translational moving of molecules, known as alpha-relaxation, and rotational movements of constituents' parts (beta-relaxation or Johari–Goldstein relaxations). In contrast to  $\alpha$ -relaxations,  $\beta$ -relaxations are generally timed by non-Arrhenius kinetics and have activation energy values

that are much smaller than those of  $\alpha$ -relaxations ( $E_a=5-12\text{kcal/mol}$  for beta-relaxation), and can be detected at 30-50°K below  $T_g$  (Johari and Goldstein 1970). Alpha-relaxations got their name because of their typical appearance at a lower frequency in dielectric relaxation studies (Johari 1973).

As glass proceeds towards an equilibrium, enthalpy decreases, free volume decreases and structural order increases, i.e. configurational entropy decreases. Since the initial state has higher enthalpy than the equilibrium state, heat is given off during relaxation.

Freshly made glass may be kept at a chosen temperature, below  $T_g$  (Figure 4). Then term “annealing” is used for planned and wanted structural changes, while term “aging” is for structural relaxation which takes place regardless experiment proceeding, usually unwanted. During annealing the stress induced by vitrification is being removed.

Enthalpy value of a glass depends on the temperature treatment of the substance (thermal history). Different ways of production result in glass of different thermodynamic properties. For example, milling of a crystalline phase may produce a glass with twice as great heat capacity value versus quenching the melt (Tsukushi et al. 1994).

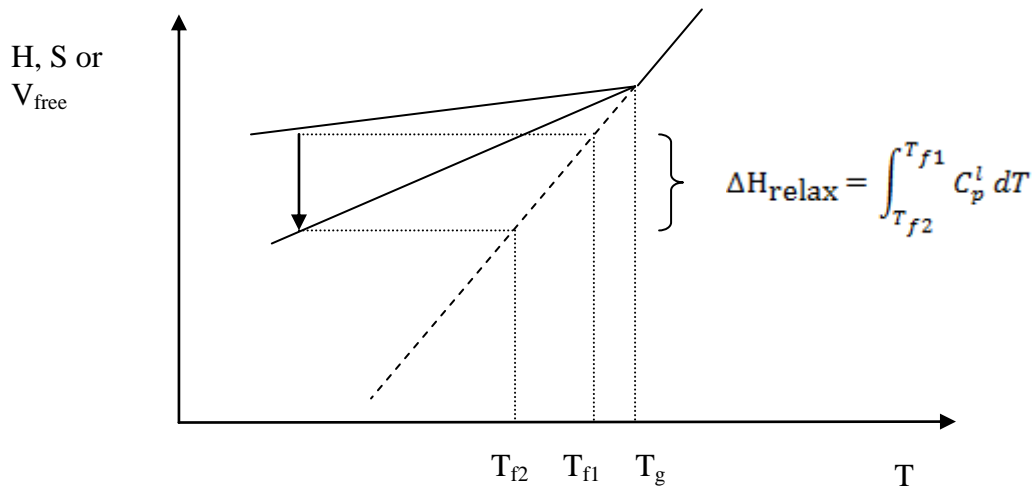


Figure 4. Enthalpy of a relaxation process. As glass relaxes toward an equilibrium, enthalpy change can be estimated through heat capacity measurements. Fictive temperature experiences a reduction as well.  $T_g$  represents glass transition temperature,  $T_{f1}$  is the fictive temperature of freshly prepared glass,  $T_{f2}$  is the fictive temperature of an annealed glass.

The possibility that not all the enthalpy of a glass is exactly configurational in nature was studied by Chang et al (Chang et al 1967). They compared freshly made (quenched) diethyl phthalate glass (with higher entropy) to annealed glass (lower entropy). These authors hypothesized that vibrational frequencies in the samples could be different. The part of the entropy difference, which arises from different vibrational frequencies, is expected to vanish as temperature approaches 0K. Only that part of the entropy, which stems from configurational mode, would be available at 0K. The results of the study suggest that non-configurational contributors have a mild effect on the excess thermodynamic qualities of a glass.

## 2.4 Evaluation of molecular mobility

The extent and the type of molecular motions strongly influence physical properties of any material. In a glass there is kinetic and thermodynamic driving force for molecular structure change towards an equilibrium. Molecular mobility can be quantified using relaxation time parameter,  $\tau$ . The parameter generally reflects the changes in thermodynamic properties of material at chosen temperature. For example, if the relaxation time is estimated to be 100s, this means that the thermodynamic properties (i.e. enthalpy) of materials will reach equilibrium ones within 100 seconds.

### 2.4.1 Average relaxation time

Average relaxation time can be estimated using enthalpy relaxation measurements. When a glass is allowed to relax there is some heat being released. The amount of decrease in enthalpy is related to the molecular mobility at the temperature. Using different experiment times the enthalpy change versus annealing time can be evaluated. From the data, the average relaxation time can be estimated at any given temperature.

Conventional DSC can be used for evaluation of average relaxation time. The procedure contains several steps and finally the data is fitted into Kohlrausch-Williams-Watts (KWW) equation, where both average relaxation time ( $\tau$ ) and the corresponding distribution parameter ( $\beta$ ) are estimated:

$$\frac{\Delta H_{t,T}}{\Delta H_{max}} = 1 - \exp \left( -\left(\frac{t}{\tau}\right)^\beta \right) \quad (2)$$

In many cases the equation has been used in modelling the relaxation behaviour of glass-forming systems.

Firstly, enthalpy relaxation ( $\Delta H_{l,T}$ ) is determined. When material is heated through glass transition region after being stored at chosen temperature below  $T_g$  for desired time, an additional endotherm can be detected at DSC scan in the endset of the transition. When compared to the freshly made glass DSC scan, the endotherm provides an estimate for enthalpy loss during the annealing (Figure 5). Samples in the experiment should have equal thermal history differing by the annealing only, since the degree of enthalpy relaxation depends on the mechanical and thermal conditions during the glass manufacture and storage (Seyler 1994).

Secondly, maximum enthalpy available for relaxation ( $\Delta H_{max}$ ) is determined, using the following equation:

$$\Delta H_{max,T} = \int_T^{T_g} \Delta C_p(T_g), \quad (3)$$

where  $\Delta C_p(T_g)$  heat capacity change at  $T_g$  and  $T$  is the annealing temperature.

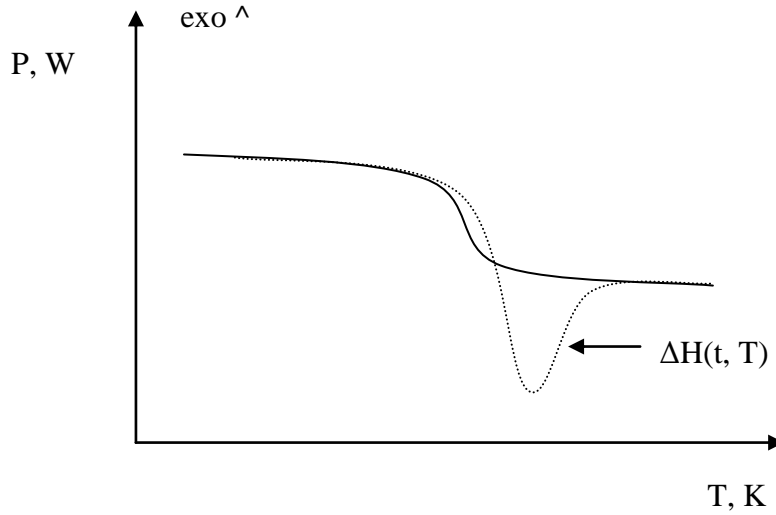


Figure 5. Determination of enthalpy relaxation using DSC scan. Dotted line represents annealed sample, continuous line is freshly made glass.

Using the equation (2) distribution parameter ( $\beta$ ) can be estimated. It is the extent to which the data deviates from a true exponential function, and with  $\beta=1$  the result would be the true exponential function. It is generally called the stretching parameter. The parameter is related

to the cooperativity associated with the structural relaxation in glasses (Rendell et al. 1991). The parameter is inversely proportional to the width of the distribution of relaxation times. It is a measure of the distribution of relaxation times (Lindsey and Patterson 1980).

The KWW equation (equation 2) contains two variables,  $\tau_{\text{KWW}}$  and  $\beta_{\text{KWW}}$ . Both of them are necessary to describe non-exponential relaxation data using the KWW equation. In any situation where  $\beta_{\text{KWW}}$  has a value significantly less than unity (i.e.,  $<0.9$ ), a direct comparison of two  $\tau_{\text{KWW}}$  values is only appropriate when the accompanying  $\beta_{\text{KWW}}$  values are similar (Cowie et al. 1998).

Average relaxation time provides an estimate of material's likely behaviour under chosen conditions (which can be a measure for the shelf life of the pharmaceutical product). For pharmaceutical use of amorphous material, relaxation time of 2-3 years is required. Experiments, based on the KWW approach, would take very long time to show the relaxation time of the magnitude. Another shortcoming of the method is that it does not describe molecular motions in the glass. One should also bear in mind the fact that the  $\tau_{\text{KWW}}$  is assumed to be constant during relaxation process.

#### 2.4.2. Relaxation time at a given temperature.

Relaxation time varies with temperature. Above  $T_g$   $\tau$  follows non-Arrhenius kinetic (Ediger et al. 1996). At  $T_g$   $\tau$  is said to be  $10^2$ s. Below  $T_g$   $\tau$  changes as function of annealing time and is impacted by thermal history of the glass. In these considerations the measure of molecular mobility is an transient feature of a glass. Pharmaceutical use of a glass requires relaxation time of about two years (this corresponds to a drug's shelf life), which is accomplishable well below  $T_g$ .

Relaxation time of a glass tends to increase as relaxation process proceeds. Adam-Gibbs theory is most accepted in evaluation of the dependence. According to the theory, a liquid consists of regions that can rearrange as units, cooperatively rearranging regions, when heat is being given to the system or removed from the system. The size of the unit is determined by configurational entropy, and varies with change in temperature. At high temperatures configurational entropy has a big value and the unit size is small. As temperature is lowered,



the configurational entropy is reduced and the size of the unit grows. Loss of configurational entropy means increase in relaxation time.

$$\tau = \tau_0 \exp\left(\frac{\Delta\mu s_c}{k_B T S_c(T)}\right) \quad (4)$$

where  $\tau$  is the relaxation time,  $\tau_0$  is the pre-exponential factor,  $T$  is the temperature,  $S_c(T)$  is the configurational entropy at temperature  $T$  and  $k_B$  is Boltzmann's constant. The terms  $s_c$  and  $\Delta\mu$  are the entropy of the smallest cooperatively rearranging region and the activation energy of cooperative rearrangement respectively. These are properties of the substance at hand.

The theory assumes that the relaxation time change is entirely dependent on configurational entropy.

The Vogel-Tamman-Fulcher (VTF) equation was derived empirically from the observed behaviour of liquids. One of its forms is:

$$\tau(T) = \tau_0 \exp\left(\frac{B}{T - C}\right) \quad (5)$$

where  $\tau_0$  ( $10^{-14}$ s) is relaxation time constant of unrestricted material at infinitely high temperature,  $B$  is related to fragility of glass, and  $C$  is a temperature at which the average molecular mobility is expected to approach zero,  $T_K$ . Parameter  $B$  is a characteristic of the material at hand, and can therefore be evaluated completely from the liquid state above  $T_g$ . In many cases the equation may be used to evaluate the temperature dependence of molecular motions below  $T_g$  (Ediger et al. 1996).

## 2.5 Fragility

Excess configuration entropy (which can be evaluated from heat capacity measurements) changes as function of temperature and time according to the type of material at hand, as amorphous material experiences structural and orientational changes. To quantify and compare different glass formers one may use fragility values.

At  $T_g$  heat capacity trend experiences changes from liquid-like to crystal-like (Angell 1995). Configurational entropy change during vitrification can be significant. In this case the observed excess thermodynamic quality in glassy state is close to the one of crystal. On further cooling the structure of the glass does not change much. The molecular mobility

change with temperature is small. Strong materials are said to have a built-in resistance to structural change. They show little reorganization despite wide change in temperature.

On the other hand, in some glasses the observed excess thermodynamic quality is close to the one of supercooled liquid (corresponding change in  $C_p$  at  $T_g$  is little). The molecular mobility change with temperature is more pronounced (fragile material). In these considerations one can conclude that less fragile material need lower storage temperatures than more fragile one. A comparison of strong and fragile material physical properties is presented in Table 1.

Table 1. A comparison of strong and fragile material physical properties.

	Fragile	Strong
$\Delta C_p$ at $T_g$	large	small
$T_m/T_g$	1-1,5	1,5 or greater
$\beta$ -value from KWW equation	$\ll 1$	$\sim 1$
Increase in $\tau$ during relaxation	more rapid	less rapid
Heating rate dependence of $T_g$ [*]	pronounced	less significant

\* (Crowley and Zografi 2001)

### 3. METHODS OF PRODUCTION OF AMORPHOUS MATERIAL

#### 3.1 Routes of production of amorphous material in pharmaceuticals

In pharmaceuticals amorphous solid can be produced either intentionally or unintentionally. Intentional production is used, for example, to improve the dissolution rate of poorly soluble compounds (Law et al. 2001), to stabilize the structure of proteins, (Carpenter et al. 1997), or to improve the mechanical properties of excipients (e.g., lactose). Commonly employed techniques include quenching of melts, rapid precipitation by antisolvent addition, freeze-drying (Pikal 1990) and spray-drying (Broadhead et al. 1992). Dehydration of crystalline hydrates can result in the amorphous state of organic solids (Saleki-Gerhardt et al. 1995). Although quenching of a melt is not a common way to produce amorphous solid on the large scale production in pharmaceutical industry, this technique is often used in laboratory experiments.

Unintentional introduction of amorphous phases can result from general manufacturing procedures of pharmaceuticals, such as coating, granulation, drying, milling, and compression. The presence of amorphous regions, even in small quantities, can exhibit a significant influence on the physical and chemical stability of pharmaceutical products (Hancock and Zografi 1997). Therefore, a consistent performance of a pharmaceutical product can be ensured by a profound understanding of properties of the amorphous state.

### 3.2 Freeze-drying

For some pharmaceutical formulations freeze-drying or lyophilisation is the technique of choice. It allows to stabilize heat and water labile substances, and to improve bioavailability of poorly soluble drugs. Sterility issues and foreign particles control are relatively simple to consider in freeze-drying. Accurate sterile dosing into final product containers is straightforward. Since freeze-drying cycle is performed at lower temperatures than spray-drying, it can be addressed as less destructive (Pikal 1990). Some pharmaceutical applications of freeze-drying include manufacturing of rapidly disintegrating tablets (Corveleyn and Remon 1997), lyophilized dry emulsion tablets for oral administration (Corveleyn and Remon 1998), vaginal suppository (Brummer et al. 1997), nasal dose delivery systems (Pereswetoff-Morath and Edman 1995).

Although freeze-drying is an expensive, time-consuming and a batch process, it is often the method of choice for protein formulations. Because there is no air-water interface, proteins in freeze-dried formulation are less susceptible to stresses during handling, shipping and storage. Translational motion of the proteins is comprehensively reduced. As a consequence, proteins collisions are also reduced and, therefore, proteins aggregation is often reduced as compared to liquid formulations. Finally, chemical stability is also generally improved in freeze-dried formulations (Chang et al. 1996).

Choice of excipients is crucial for lyophilized formulation. But even if a formulation has the potential to form a stable product in the dried solid form, only a carefully planned freeze-drying process may realize this potential. Physical properties of the formulation dictate freeze-drying cycle parameters such as pressure, temperature and duration. Efficiency of each stage and successful final product can be ensured by deliberate lyophilisation process design.

### 3.2.1 Freezing step

Freezing is essentially the first step of a freeze-drying cycle. During freezing ice crystals of pure water are formed. The product can be said to separate into ice crystals and solute, which concentrates at freezing (removing water in form of ice). The temperature at which ice crystals start to form is known as the ice nucleation temperature. The ice nucleation temperature is influenced by formulation and process parameters.

The structure of freeze-dried product is determined to a large extent by the freezing process. Ice crystal morphology and size distribution are defined by freezing method, which in turn affects primary drying rate (Pikal 1990a), secondary drying rate (Pikal et al. 1983), and product surface area (Hsu et al. 1995) of the lyophilized system. Ice crystal size is dictated by degree of supercooling, with higher supercooling resulting in lower ice nucleation temperature and smaller ice crystals. Sublimation of ice during second stage of freeze-drying process leaves behind a porous structure (cake). Structures with better interconnected and more direct vapour flow paths toward the top of the cake dry faster. Searles et al. (Searles et al. 2001) showed that every 1°C decrease in ice nucleation temperature result in an approximate 3% increase in primary drying time.

To ensure full solidification during freezing step, the product temperature is reduced to a point below the formulation glass transition temperature of the maximally concentrated solute,  $T_g'$  (or freeze concentrate). It is generally known that the glass transition temperature of amorphous solid depends on the moisture content. State diagram or so called supplemented phase diagram (an example is presented in Figure 6) can be used to describe changes in glass transition as a function of water content or different degrees of freeze-concentration (Roos and Karel 1991). The glass transition dependence on water content may be the source of differences in reported glass transition temperatures.

Moderate rate of cooling during freezing step provides temperature reduction of the product, freezing of water and consequent sugar concentration in a manner of equilibrium freezing curve (see Figure 6). In case of disaccharides co-crystallization of sugar at  $T_e$  is hindered by complexity of molecule and viscosity of the product (Roos and Karel 1991). The freeze-concentration continues past  $T_e$  into a non-equilibrium state of supersaturated solution until a point is reached, where the solution is maximally freeze-concentrated ( $T_g'$ ). It has been

discussed in the previous chapter, the point of glass transition has kinetic and thermodynamic features. The solidification of the product during freezing step results in a structure, where unfrozen (or amorphous) phase is a continuous phase surrounding ice crystal areas in frozen product. A SEM image of amorphous solid left behind in the end of freeze-drying process is given in Figure 7.

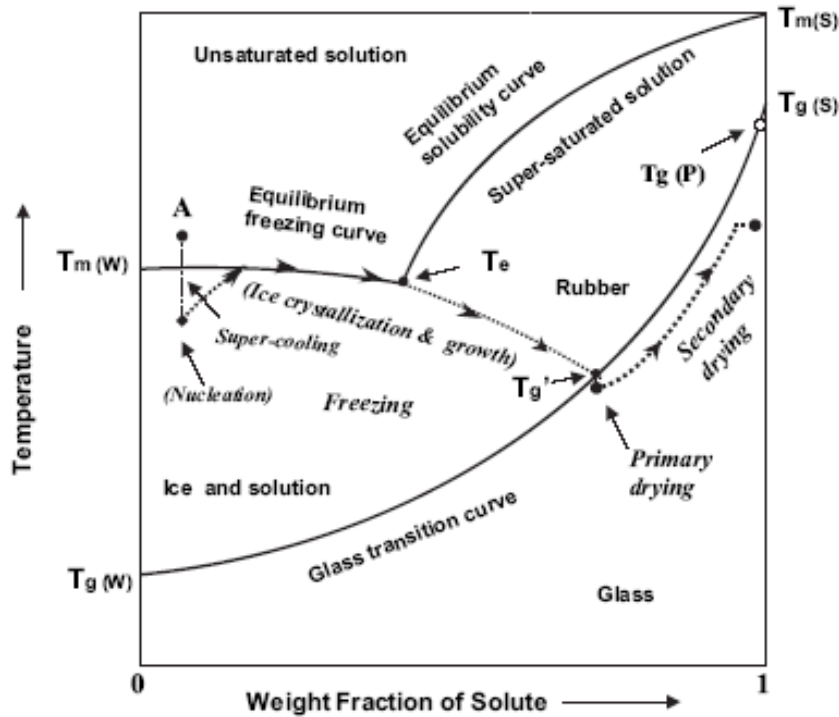


Figure 6. Supplemented phase diagram for a binary formulation system where the solute (S), such as sugar, does not crystallize during freeze-drying. Arrows illustrate freeze-drying process. A represents formulation aqueous solution;  $T_m(W)$  and  $T_m(S)$  are melting temperatures of water and solute, respectively;  $T_g(W)$  and  $T_g(S)$  are glass transition temperatures of water and solute, respectively;  $T_g'$  and  $T_g(P)$  are glass transition temperatures of freeze concentrate of the formulation and the freeze-dried product, respectively;  $T_e$  denotes the eutectic temperature. Reproduced from ref. Liu 2006.

Fast cooling can result in lower solute concentrations, when less water is removed from the solution in form of ice. Failure to crystallize sufficient amount of water can result in depression of the  $T_g'$  and compromising storage stability of the formulation afterwards. The reduction of  $T_g'$  as a result of increased water content can be attributed to the low  $T_g$  ( $-135^{\circ}\text{C}$ ) of pure water.

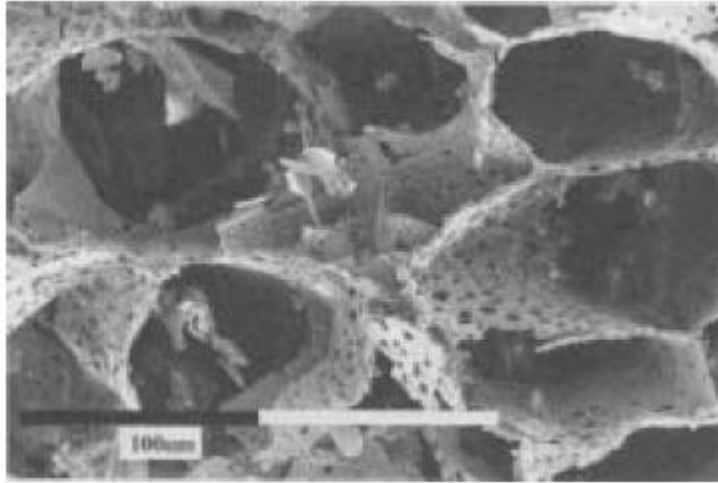


Figure 7. Microstructure of lyophilized trehalose formulation observed using SEM: the pores (diameter <100 micrometres) were left behind by the ice crystals formed during the freezing process. Reproduced from ref. Overcashier et al. 1999.

A practical technique to optimize ice crystal size distribution during freezing is to incorporate an annealing step (Searles et al. 2001). The purpose is to facilitate crystallization of ice. Frozen samples are maintained during some period of time at a temperature above the formulation's glass transition temperature ( $T_g'$ ) but still below the solution's freezing point. Then the average ice particle size grows: smaller ice crystals join those of larger sizes. The phenomenon name is Ostwald ripening (Voorhees 1984). Annealing does not only help to create an elegant cake appearance, but also may accelerate the freeze-drying process. Disadvantages include experimental-based identification of optimal conditions for annealing (temperature and length). Secondly, high molecular mobility at the temperature above  $T_g'$  of the formulation may lead to significant problems concerning stability of the system.

State diagram in Figure 6 considers a binary system of a sugar and water. Real systems are more complex. However, often main carbohydrate, which governs the glass transition, can be indicated. For example, the glass transition of milk powders followed closely that of lactose (Jouppila and Roos 1994). When lactose was hydrolysed to its glucose and galactose counterparts, a comprehensively lower glass transition and critical water activity and water content were observed.

In another research on cytoplasm of desiccation tolerant plants (Wolkers et al. 1998) it was suggested that the carbohydrates that are present in the cytoplasm are the primary factors contributing to the glassy state.

After freezing the product should be in solid state. That means the water should be frozen, and the sugar should be in amorphous form. It can be achieved by keeping the formulation at the target temperature, i.e. below  $T_g'$  of amorphous system, for long enough to allow complete solidification of the product. The freezing time depends on fill volume (Pikal 1990). The final temperature is held for 1 h if the fill depth is less than or equal to 1 cm or 2 h if the fill depth is greater than 1 cm (Tang and Pikal 2004).

### 3.2.2 Primary drying

Primary drying, or ice sublimation, is the second stage in freeze-drying process. The chamber pressure and the shelf temperature are adjusted to allow ice sublimation from the product. During primary drying the chamber pressure is kept below the vapour pressure of ice allowing the sublimed water vapour to transfer from the product to the condenser, where it is crystallized. Primary drying is the most time-consuming step of freeze-drying process and optimization of this step represents the biggest potential for process design improvement (Pikal 1990b).

The prime concern on this step is to optimize the product temperature ( $T_p$ ). It is difficult to control directly.  $T_g'$  of the formulation (and in case of eutectic mixture,  $T_c$ ) provides an estimate for temperature regime during primary drying, where the product temperature should be a few degrees below the critical value to maintain product's desired characteristics. It has been studied (Pikal 1990a) that higher temperature regimes result in faster drying, where each 1°C increase in product temperature causes reduction in primary drying time by about 13%. However, with temperature choice close to  $T_g'$ , the product stability can be challenged. Therefore, choice of product temperature for primary drying is a balance between achieving the shortest possible drying time, which is important for the process optimization, and the product stability during and after drying.

The pressure of the chamber during primary drying should be low enough to allow ice sublimation. It is generally accepted, that the lower the chamber pressure, the higher the sublimation rate. However, very low chamber pressure may result in inefficient heat transfer required for sublimation (Pikal et al. 1984). Consequently, the choice of chamber pressure

represents a compromise between fast sublimation rate and efficient heat transfer for sublimation.

Shelf temperature during primary drying is another adjustable operating condition, which can improve sublimation rate. Sublimation of water requires energy (the latent heat of sublimation is 2840 kJ/kg for ice) and consequently reduces the product temperature, so heat supply is needed to maintain continuous ice sublimation. Shelf temperature is raised for the purpose. However, the shelf temperature cannot be raised freely. Keeping the product temperature below formulation's  $T_g$  is important to avoid collapse in the product.

During the primary drying all the ice is removed from the product. The end point of the stage can be determined by ice sublimation ceasing, consequently, there is no heat removal by sublimation. At this point the product temperature raises to the shelf temperature level. Vapour composition analysis can provide another way to determine the end point of primary drying, when there is a change from essentially all water vapour during primary drying to mostly air or nitrogen (Pikal et al. 1984).

### 3.2.3 Secondary drying

Secondary drying is the third stage of freeze-drying process. It starts whenever ice has been removed from the frozen formulation. The product's structure needs to be maintained all the time during either primary or secondary drying by careful validation of temperature program. After the primary drying stage there is no ice left in the product, but there is a pronounced amount of water left in the solute phase. The residual water may be absorbed on the surface of crystalline solids (if there are any), as a hydrate form of crystals or water can be included into amorphous matrix in form a solid solution. The water amount is reduced during the secondary drying. Usually the temperature is raised and pressure remains low for the purpose. Some unfrozen water removal can occur during primary drying after the ice is sublimed from the region, but the most of unfrozen water evaporation occurs after primary drying at elevated temperature.

The temperature regime should be validated with care. During drying the product water content is reduced. It can be seen from the state diagram (Figure 6), formulation  $T_g$  depends strongly on water content and raises significantly during the secondary drying. The



temperature elevation at the stage should be based on moisture desorption kinetics. Careful estimation of moisture desorption isotherm can provide an opportunity for the stage optimization.

The endpoint of secondary drying is preferably estimated without interrupting the drying process. Residual moisture can be measured using Karl Fischer titration, thermal gravimetric analysis or near IR spectroscopy (Kamat et al. 1989). In most cases samples for inspection are removed from the chamber without interrupting the drying process, using a sample thief.

#### 4. METHODS OF CHARACTERIZATION OF AMORPHOUS MATERIAL

Among all the techniques available to study amorphous materials, the most commonly used appears to be differential scanning calorimetry. Thermodynamic properties (estimated by means of DSC) of amorphous solids are of great importance for drug development. Study of thermal events can provide an insight into the dynamics and stability specifications of formulation in question.

Glass transition is a characteristic feature of any amorphous material. At the transition molecular mobility changes dramatically. Consequently, a change in many physical parameters of the material at the transition can be observed: changes in volume, density, heat capacity, viscoelastic modulus, electrical permittivity and refractive index can be investigated.

Techniques for monitoring density and volume change of amorphous material have not been commonly applied within pharmaceutical industry. The reason for that is probably due to experimental difficulties.

A number of techniques (some of them are described in the present chapter) have been used to identify amorphous materials. For some of them there have been developed methods to identify the amount of amorphous content. Most of the methods are still under development.

#### 4.1 Diffraction techniques

There is no long-range order for molecules in amorphous material. Diffraction techniques allow to detect and quantify molecular order in any system. The techniques are non-destructive and accurate, therefore they are often used in description of pharmaceutically relevant materials. In monitoring non-crystalline systems using conventional X-ray powder diffraction accuracy of as low as about 5%-10% of non-crystallinity can be obtained (Saleki-Gerhardt et al. 1994). The quantification is based on calibration curve. The equation for the curve is obtained by integration of intensity of a few strongest peaks of 100% crystalline material and by comparison of the values to the intensities of the peaks of samples with different amounts of crystallinity. The detection limit can be improved using special optics and advanced software (Chen et al 2001). The authors reported detection limit of 0.37% of amorphous content.

The wavelength of the electromagnetic radiation used in X-ray powder diffraction technique is of order of interatomic distances. 1.54 angstroms is often used and the length of C-C bond is about 1.5 angstroms. The regular arrangement of atoms in a crystal result in certain wave directions reinforcement (wave interference), and some directions neutralization according to the similarity of wavelengths to the distances between the atoms or molecules in crystal. The resulting curve of X-ray diffraction pattern can be told to be a fingerprint of the crystal under the study. However, one should bear in mind that diffraction techniques can only indicate order in the system, and therefore disorder is only hinted. X-rays penetrate the whole sample and thus the sample average is depicted in the X-ray diffraction pattern. Another issue to consider could be that small crystals do not produce as “crystalline” diffractograms as bigger crystals because of the higher proportion of surface (and hence nonplanar structure).

#### 4.2 Spectroscopic techniques

Spectroscopic techniques represent another example of non-destructive investigation methods. Characterization of many different pharmaceutical systems can benefit from their high structural resolution. Spectroscopic techniques are not commonly employed in studying of amorphous materials, but some steps in the direction have been made. In the following there are examples of using Nuclear magnetic resonance (NMR) and infrared (IR) spectroscopy in determination of the glass transition temperature of amorphous materials. However, the

interpretation of data obtained from spectroscopic measurements is often quite complex and may require additional experiments using other techniques.

With NMR, the magnetic properties of atomic nuclei are studied, where mobility of molecules can be estimated by monitoring the relaxation profile of the NMR active nuclei, for example,  $^{13}\text{C}$ . Glass transition involves a distinct change in molecular mobility and with NMR the motional properties of molecules can be studied. During NMR experiment the spin-spin relaxation can be monitored. It was found that the profile of the spin-spin relaxation time of the 'rigid' component was related to the glass transition (Kalicevsky 1992).

Another research (Ruan et al 1998) investigated the use of the low field NMR technique in studying glass transition in food polymers. The result of the NMR study was shown in a curve, where spin-spin relaxation times were plotted as function of temperature. The curve was found to be "L"-shaped with glass transition temperature being the "turning point" in the curve. Changes in spin-spin relaxation times as function of temperature are generally associated with the thermal mobility of the molecules. The turning point in the curve determines the glass transition event through the increased mobility of the labelled nuclei.

Harmonic oscillations associated with the stretching and bending of bonds can be investigated using electromagnetic radiation of infrared region. The masses of vibrating or rotating atoms as well as bond strength determine the frequency of the infrared absorption. Thermal transitions affect hydrogen bonding in the sample. Precise position and shape of the peaks (i.e. broadening of absorbance bands) in spectrum can be indicative of changing in the hydrogen bonding structure. In some cases spectroscopic instruments have the possibility to adapt heating cells (in situ dynamic analysis). Spectral data obtained indicate the changes in the sample at chosen temperature interval.

Wolkers et al (Wolkers et al. 1998) studied the IR spectrum of amorphous sugars and found that the peak wavenumber for the hydroxyl groups stretching vibrations increased linearly as function of temperature. Furthermore, a distinct change in the linear dependence at  $T_g$  was observed. Generally, the peak position depends on the degree of restriction of the bond, which reflects the degree of interactions with atoms in the neighbourhood. Therefore, the positive shift in the peak position for the O-H stretching vibration as temperature increases means that the extent of interactions with neighbour molecules decreases. And since hydrogen bonds

keep the amorphous matrix of a sugar in place, it was stated that the extent of formation of hydrogen bonds decreases.

Amorphous content of a sample can be estimated using near IR spectroscopy (Hogan and Buckton 2001). The evaluation is performed using calibration curve, which is obtained through comparison of IR spectra of completely crystalline and completely amorphous forms of the material. The method demands well-resolved bands in the spectra of amorphous and crystalline phases. The method was estimated to be accurate to within 1% w/w amorphous content.

#### 4.3. Dynamic vapour sorption

The moisture sorption profile can be used in identifying amorphous material due to tendency of the metastable amorphous material to moisture-induced recrystallization. Moisture sorption isotherm (change in mass as function of RH) produced during a sorption–desorption cycle shows water vapour sorption profile of the sample between 0 and 100% RH at chosen temperature. For an amorphous solid a significant increase in moisture uptake can be observed at relatively low humidity levels with consequent recrystallization on further increasing of the water vapour pressure (Elamin et al. 1995). The recrystallization is accompanied by a weight loss of the sample. The characteristic behaviour is believed to be related to the extraction of water during the recrystallization process, where anhydrate formation is accompanied by a dramatic weight loss. In case of a hydrate formation the weight loss is generally less pronounced.

#### 4.4 Dielectric relaxation measurements

Dielectric relaxation measurements have been proved sensitive to the glass transition event (Duddu and Sokolski 1995). The technique allows to monitor microscopic “viscosity” of the system, and activation energies for transitions can be estimated. During the experiment changing electric field is applied to the sample. The motions of dipoles are detected as a phase shift relative to the time scale and frequency used. Dielectric permittivity is the response of material estimated as a function of temperature. The glass transition is determined through an abrupt change in dielectric permittivity of the sample. However, the material under the study must have dielectric properties. Some materials, for example, have either too high response

(such as strong electrolyte solutions or metals) or too low response (such as solid hydrocarbons) (Craig 1992). The results of the measurements are sensitive to moisture content of the sample and some materials exhibit isomerization during the experiment, which can have an impact on relaxation profile (Noel et al. 2000). Sample requirements are relatively high (more than 100 mg) and sample preparation can sometimes be difficult.

#### 4.5 Thermal techniques

Enthalpy of amorphous solid is significantly higher than that of correspondent crystalline form. Enthalpy studies are commonly performed using thermal techniques. Thermal techniques estimate the relationship between a property of the sample and its temperature. Important thermal analysis techniques applicable to amorphous solids studies are differential scanning calorimetry (DSC), thermomechanical analysis (TMA) and dynamic mechanical analysis (DMA).

##### 4.5.1 Thermomechanical analysis and dynamic mechanical analysis

Thermomechanical analysis (TMA) monitors the deformation (dimensional changes) of a sample as function of temperature. During TMA experiment the sample is subjected to a nonoscillatory constant, increasing or modulated force (stress or load) and dimensional changes are monitored.

Using TMA it is possible to detect thermal events, estimate temperatures of the events, determine deformation step height and estimate expansion coefficients. Typical TMA curve shows a dimension (i.e. thickness, for example in micrometres) of the sample as function of temperature. Then the  $T_g$  is represented by a change in resistance to penetration. The thermal expansion coefficient increases at the glass transition resulting in a significant change in the slope of the curve, which results in a change in slope of the specific volume vs. temperature curve at the glass transition temperature (Biliaderis et al. 1986).

Another approach to define glass transition was used by Hancock et al (Hancock et al. 1999), where viscosity of amorphous indomethacin samples was determined. The TMA curve showed probe penetration depth as function of experimental time at chosen temperature. Then the viscosity was calculated as simple function of the probe diameter, applied load and

experimentally determined penetration rate. Quantification of glass transition parameters requires, however, previous knowledge of viscosity dynamics for the material at hand.

Dynamic mechanical analysis (DMA) provides information about viscoelastic properties of the sample as function of time, temperature and frequency. In DMA the sample is subjected to a changing (oscillatory) mechanical stress. The applied force amplitude, displacement (deformation of the sample) amplitude and phase difference between the force and displacement signal can be monitored during the experiment.

A number of different curves can be obtained from DMA experiment. Glass transition can be observed through measuring of storage modulus and the loss factor. Modulus can be defined as the resistance of a material to deformation (in Pa). The storage modulus is proportional to the mechanical energy stored in the sample during the stress period. In Figure 8, there is a geometric relationship between the important three moduli and the loss angle,  $\delta$ .

The loss modulus  $M''$  is the energy lost as heat during a stress cycle in the material. Viscous behaviour is characterized by a high loss modulus. The loss factor,  $\tan \delta$ , represents the ratio of the elastic and the viscous properties. A high degree of non-elastic deformation is defined by a high value of the loss factor.

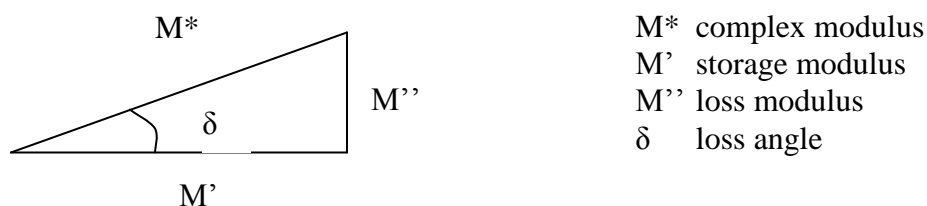


Figure 8. A geometric representation of the three moduli and the loss angle,  $\delta$ . The values are used to evaluate viscoelastic properties of the sample from DMA experiment.

The mechanical properties of sample changes markedly in the region of glass transition (Kim et al. 1994). The mobility of molecules increases greatly at  $T_g$ . This is accompanied by corresponding decrease in the characteristic modulus. The DMA curve can display the storage modulus (in Pa) and the loss factor as function of temperature. For amorphous material the storage modulus is of the order of several GPa. In the region of glass transition the parameter decreases typically by several orders. Another indicator of glass transition is the dynamics of

the loss factor (a distinct maximum can be observed). The great change in the mentioned above parameters means that the technique is very sensitive to glass transition. The measurement can be performed for the material with little change in  $C_p$  at  $T_g$ , which would challenge traditional DSC monitoring.

#### 4.5.2 Differential scanning calorimetry

In a DSC experiment the heat flow that occurs in a sample is measured when the temperature of the sample is programmed. The temperature program may involve heating or cooling or holding the sample isothermally or any sequence of these. Applicable to amorphous state studying, the technique can be used for example to detect endothermic and exothermic events, measure peak areas (transition and reaction enthalpies), identify the key temperatures for the peaks or other events, and estimate specific heat capacity.

DSC is often used in studying of pharmaceuticals because of its convenience, speed, small sample requirements, standard procedures and for the reason that it can be effectively used at low temperatures. Physical transitions and chemical reactions can be determined quantitatively using DSC. Some applications include analysis of the melting point and enthalpy of fusion, crystallization behaviour and supercooling, solid-solid transitions and polymorphism, the glass transition of amorphous materials, chemical reactions such as thermal decomposition.

Principal approaches of DSC measurements include heat flux DSC and power compensation DSC. In heat flux DSC the temperature differential between the sample and reference is measured and the equivalent heat flow is calculated. Then at a chosen scanning rate the heat flow is estimated and displayed against temperature. In power compensation DSC a compensatory power input to one or other pan is measured in order to maintain both at the same temperature regime. Due to the scaling direction on the ordinate, power compensation DSC yields endotherms pointing upwards and exotherms downwards, while heat flux based equipment gives the opposite directions.

The glass transition is a phenomenon that can be monitored in amorphous material as a step in heat capacity curve. The glass transition temperature,  $T_g$ , the step height,  $\Delta C_p$ , and the width of glass transition can be estimated from DSC curve. With the increase of heat capacity of

amorphous material at glass transition there is a shift in DSC curve in the endothermic direction. Typically, the radius of curvature at the onset is greater than at the endset, and the curve slopes in the endothermic direction before the transition but is almost horizontal afterwards. In addition, an annealing of the sample below  $T_g$  yields an endothermic relaxation peak on the endset of transition, when the sample is heated for the first time after the annealing. This peak is not observed on cooling the sample through the glass transition, either it cannot be reproduced on immediate reheating afterwards.

Different methods (see Table 2) can be used to determine the glass transition temperature based on DSC curve. Each method yields somewhat different result. Therefore, the evaluation method and the experimental parameters should always be identified. If a large enthalpy relaxation peak is observed, greater differences are to be expected.

Table 2. Commonly employed methods for estimation of  $T_g$  from DSC thermogram.

Name of the method	A brief description of the method
Bisector method	$T_g$ is the temperature at which the bisector of the angle between the two tangents intersects the DSC curve. The method is used in the evaluation software in the laboratory experiments of the present work.
Point of inflection	$T_g$ is the temperature of the point of inflection of the DSC curve.
ASTM D 3418	$T_g$ is equal to the mean value between $T_1$ and $T_2$ , see Figure 9.

Glass transition temperature can be evaluated using different thermal techniques. However, a comparison of experimental results from different laboratories (while using the same thermal technique) is only possible when the analysis instruments are properly calibrated and the details of the measurements are identified. In addition to this, thermal pretreatment of the amorphous sample under the study is just as important as the evaluation method details.

Conventional DSC experiments can be used to quantify the amount of amorphous content in the sample. Estimation of amorphous content is performed on the basis of enthalpy differences of crystallisation and melting of the partially crystalline sample and the enthalpy of melting of the purely crystalline sample. However, the accuracy of evaluation is limited by overlapping thermal events and overall instrument sensitivity, since low amorphous content of the sample is reflected in a small thermal event in the DSC curve. The results can be improved using modulated DSC, as well as high speed DSC equipment.



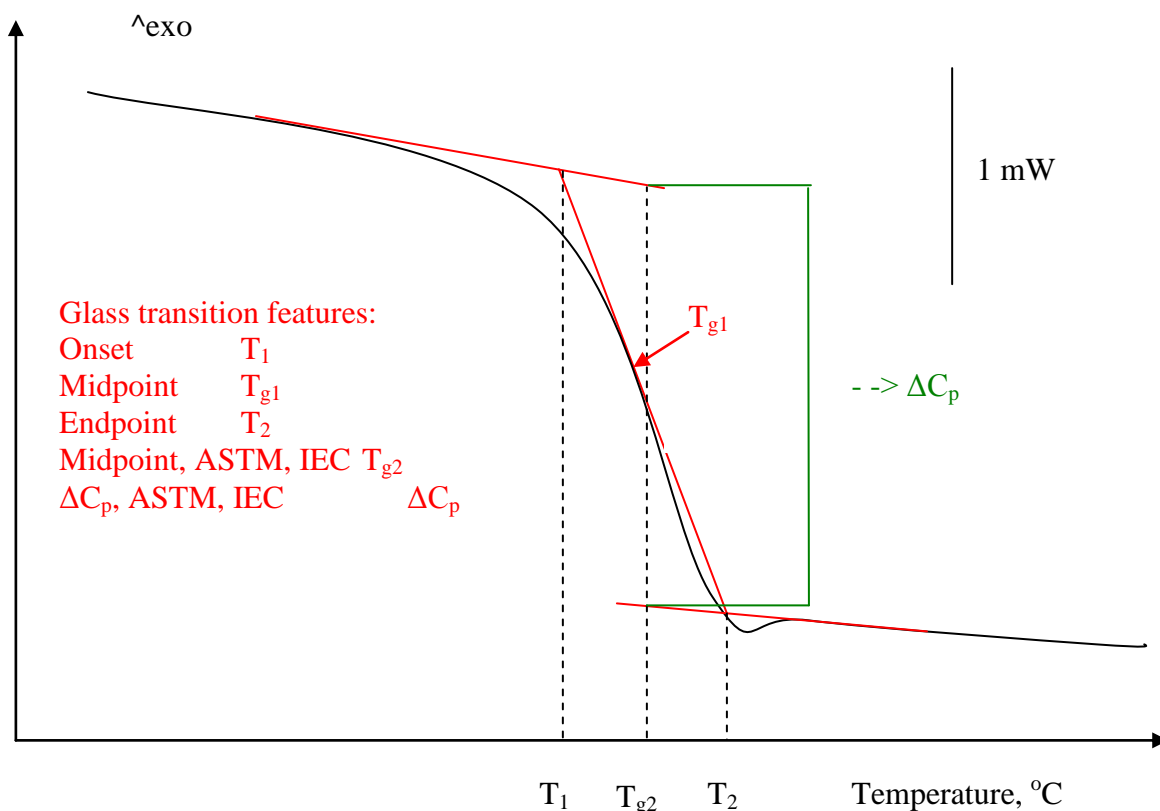


Figure 9. Schematic presentation of several glass transition characteristics.  $T_{g1}$  is the glass transition temperature defined using the angle bisector;  $T_{g2}$  is the glass transition temperature defined by ASTM D3418; width of glass transition:  $\Delta T = T_2 - T_1$ ;  $\Delta C_p$  is the step height.

#### 4.5.3 Modulated differential scanning calorimetry

Modulated DSC is a development of conventional DSC, whereby a modulation is applied to the heating or cooling signal. In conventional DSC linear heating or cooling temperature program is used. The modulation or usually sinusoidally varying temperature program allows separating the reversing and non-reversing components of thermal event under the study. The kind of signal separation is beneficial, when an overlap with other thermal events can be expected.

In principle, the total heat flow from mDSC should be consistent with the heat flow from a conventional DSC at the same heating rate. Differences can be attributed to the choice of experimental parameters (mDSC has a few more adjustable variables, such as period of modulation and temperature amplitude).

Using mDSC for glass transition studies, clear visualisation of the glass transition and relaxation endotherm can be obtained. An example of mDSC scan is presented in Figure 10.

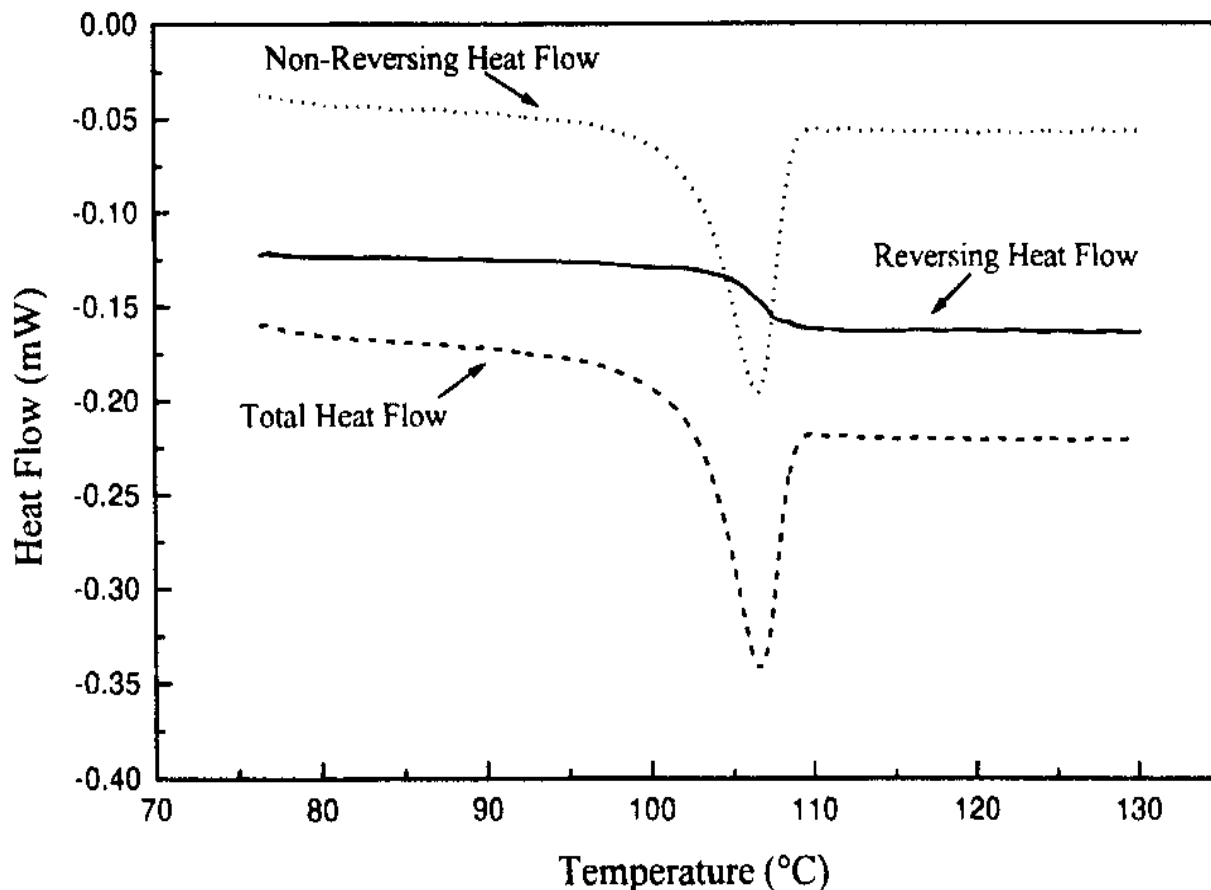


Figure 10. Modulated DSC response of amorphous saquinavir, showing the reversing, non-reversing and total heat flow signals (Royall et al. 1998).

Disadvantages, related to the technique, include the necessity to detailed control of the experimental variables. Slow scan speeds are needed so that oscillations would not disturb steady state of the sample. This would result in longer experimental times and cause the risk of annealing during the cycling process.

With mDSC mass of the sample need to be validated with care, since if the sample mass is too big, then not all the mass is following the modulation (Hill et al. 1999). The temperature oscillations need to be small, so that the kinetic response could be assumed to be is approximately linear.

It has been recently introduced to the market an advanced multi-frequency temperature modulation technique TOPEM® is an upgrade for mDSC equipment, where a large number of different frequencies can be used in a single run. In contrast, methods used before the upgrade have overlaid heating ramp with a (usually) sinusoidal temperature modulation of just one frequency.

#### 4.5.4 Isothermal microcalorimetry

As little as 1% of amorphous content in a powder can be identified using microcalorimetry (Bystrom and Briggner 1994; Briggner et al. 1994). During the kind of isothermal microcalorimetry (IMC) experiment the sample is subjected to controlled supply of water (or other chosen solvent) vapour at chosen temperature. The amount of heat released or absorbed by the sample is monitored. Due to plasticizing effect the glass transition temperature of the sample decreases and molecular motions increase on the exposure to water vapour. When  $T_g$  is reduced below the experimental temperature, the crystallization of amorphous content occurs. This is an exothermic process. The amount of heat released is proportional to the amount of amorphous content in the sample. Using the enthalpy of crystallisation (for example, calibration curve can be used), the amount of amorphous content can be quantified.

## II EXPERIMENTAL PART

### 5. THE AIM OF THE STUDY

Molecular mobility in formulation with amorphous content is believed to be the key factor of their stability. For such a formulation processing and storage conditions need to be validated to provide desired and consistent performance for the drug. Therefore, evaluating of molecular mobility is an important step in pharmaceutical product development.

Structural relaxation time ( $\tau$ ) is a measure of molecular mobility in amorphous material. Calorimetric methods have been used to estimate the parameter. In enthalpy recovery experiment (Hancock et al. 1995) enthalpy of annealed amorphous solid is evaluated using DSC. The relaxation time parameter is calculated using Kohlrausch-Williams-Watts (KWW) equation. However, one of the disadvantages of the approach includes the fact that the desired shelf-life of a pharmaceutical product is about 2-3 years. Direct estimation of relaxation time based on the approach would need exceptionally long experiments (a few years long), since there is no method available to extrapolate the results from a shorter enthalpy recovery study to the desired period of time and the dynamics of relaxation time parameter possesses both nonlinear and nonexponential features.

Evaluation of molecular mobility in the present study is based on a calorimetric approach for estimation of initial relaxation time ( $\tau_i$ ). The parameter reflects mobility in freshly made glassy matrix at chosen temperature, before any annealing. Since the desired shelf-life of a pharmaceutical product is 2-3 years, and the relaxation time parameter is temperature dependent, the temperature for estimation need to be low enough to maintain the desired characteristics of the products. When the temperature of interest is significantly below  $T_g$ , the dynamics of relaxation time does not experience theoretically meaningful changes with time. Therefore, the initial relaxation time represents an estimate of average relaxation time on the pharmaceutically relevant timescale. The technique, if valid, would provide a fast, low sample requirement and widespread instrumentation method, which can be especially applicable in preformulation.

## 6. METHOD DEVELOPMENT

Heat capacity is a thermodynamic quantity of great importance for the characterization of the amorphous state. It is experimentally accessible and is used to estimate such thermodynamic properties of a glass as entropy and enthalpy. Heat capacity change with temperature depends on the material at hand. The  $C_p$  can follow linear or a hyperbolic temperature dependence. Generally, the hyperbolic equation is more accurate way to describe the temperature dependence of  $C_p$  (Hodge 1996).

AG theory describes molecular motions on the basis of configurational entropy.

$$\tau = \tau_0 \exp [C/(TS_c)], \quad (1)$$

where  $C$  is a constant,  $T$  is temperature and  $S_c$  is configurational entropy.

Vogel-Tamman-Fulcher (VTF) equation describes molecular motions as function of temperature in equilibrium system, i.e. above  $T_g$ :

$$\tau = \tau_0 e^{\frac{DT_0}{T - T_0}}, \quad (2)$$

where the parameter  $D$  is a measure of fragility of the material (strength parameter) and  $T_0$  is the temperature at which  $\tau$  becomes infinite, a point which is theoretically related to  $T_K$ .

Equation [1] can be converted into equation [2], using the temperature dependence relation of configurational entropy in integrated form:

$$S_c = \int_{T_2}^{T_1} \left( \frac{C_p}{T} \right) dT \quad (3)$$

Fictive temperature is used to describe thermodynamic qualities of amorphous state:

$$S_c(T_1) = S_c^l(T_f) = \int_{T_0}^{T_f} \left( \frac{C_p}{T} \right) dT \quad (4)$$

Substitution of the term [4] to VTF equation [2] produces an equation for the relaxation time as a function of both the temperature and fictive temperature, i.e. it can be applied below  $T_g$ .

$$\tau = \tau_0 e^{\frac{DT_0}{T \left( 1 - \frac{T_0}{T_f} \right)}} \quad (5)$$

Fictive temperature value can be estimated from the heat capacity measurements. As it has been discussed earlier, the total enthalpy of a glass available for relaxation can be defined in terms of either  $T_f$  or  $T_g$ .

$$\Delta H_{\text{glass}}(T_1) = \int_{T_1}^{T_f} (C_p^l - C_p^x) dT = \int_{T_1}^{T_g} (C_p^l - C_p^g) dT, \quad (6)$$

where  $C_p^l$  is the heat capacity of liquid form,  $C_p^g$  is the heat capacity of glass,  $C_p^x$  is the heat capacity of crystalline form, as illustrated in Figure 12.

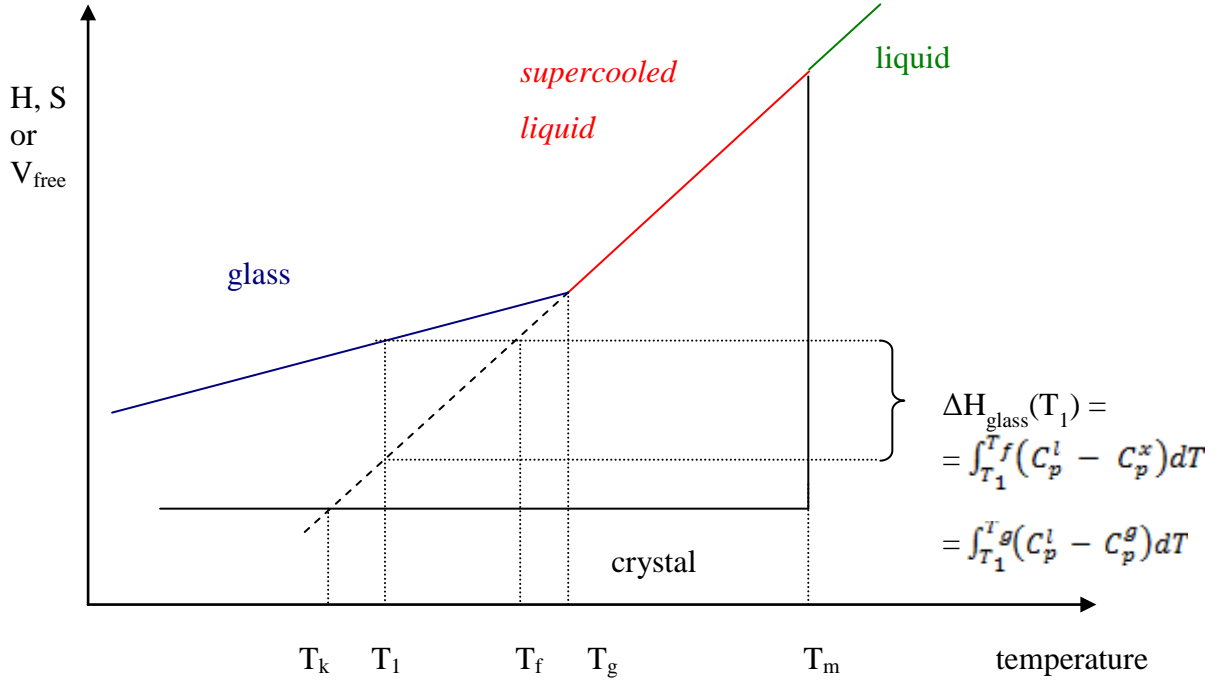


Figure 12. Schematic presentation of fictive temperature and enthalpy of a glass available for relaxation at temperature  $T_1$ . Here  $T_k$  is a point, where supercooled liquid's enthalpy is equal to crystal's one.

The equation (6) can be modified as follows:

$$T_f = T_g^\gamma \times T_1^{1-\gamma}, \quad (7)$$

where

$$\gamma = \frac{(C_p^l - C_p^g)}{(C_p^l - C_p^x)} \bigg|_{T_g} \quad (8)$$

Combining equations (5) and (7) produces following equation for relaxation time estimation:

$$\tau = \tau_0 e^{\frac{DT_0}{T(1-T_0(\frac{T}{T_g})^\gamma)}} \quad (9)$$

When heat capacity measurements are performed on amorphous solid before annealing, the measured values reflect characteristics of the material at the beginning of the relaxation process. In this case the relaxation time value is the initial relaxation time under the study,  $\tau_i$ .

The equation (9) contains two unknown parameters  $D$  and  $T_0$ . They can be defined from fragility estimation originally introduced by Angell (Böhmer et al. 1993), through steepness index  $m$ .

$$D = \frac{(\ln 10)m_{\min}^2}{m - m_{\min}} \quad (10)$$

$$T_0 = \frac{T_g (m - m_{\min})}{m} \quad (11)$$

where  $m$  is equal to the slope in a fragility plot of  $\log_{10}(\tau)$  versus  $T_g/T$  and at  $T = T_g$

$$m = \frac{d \log_{10}(\tau)}{d(T_g/T)} = \frac{E}{(\ln 10)RT_g} = \log_{10}(\tau_g / \tau_0) \quad (12)$$

The latter expression is a logarithmic version of the Arrhenius law at  $T=T_g$ .

The minimum value of  $m$  can be estimated using Eq. 12, where  $\tau_g$  is 100 sec and  $\tau_0$  equals  $10^{-14}$  s.  $\tau_0$  is relaxation time constant of unrestricted material at infinitely high temperature.

$$m_{\min} = \log_{10}(100 / 10^{-14}) = 16$$

Performing the calculations for a single temperature  $T=T_g$ , the apparent activation enthalpy for molecular motions can be derived from  $T_g$  depends on heating rate,  $q$ , (Moynihan, 1974) following the relation:

$$\frac{-\Delta E_{T_g}}{R} = \frac{d(\ln q)}{d(1/T_g)} \quad (13)$$

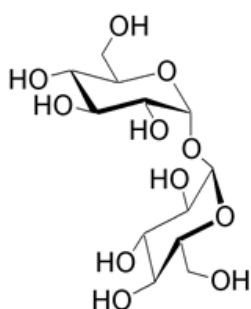
where  $R$  is gas constant.

## 7. MATERIALS AND METHODS

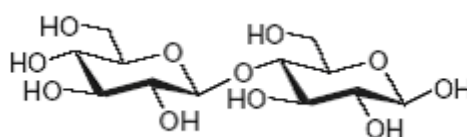
D-trehalose, D-sucrose, D-cellobiose and D-melibiose were purchased from Sigma-Aldrich (MO, USA). The molecular structure of the disaccharides is presented in Figure 11. Purified water was used to produce solutions for lyophilisation with 10 mg/ml concentration. One ml of each solution was measured into blow-molded 10 ml vials. Rubber stoppers were put loosely on the vials to allow diffusion of water vapour during freeze-drying. Lyostar II freeze dryer (SP Industries Inc., Warminster, USA) was used to produce lyophilized disaccharides.

The vials were located randomly on the shelves. Equilibration of 30 min at 5°C was used prior to freezing step. The temperature was then lowered to -45°C and kept for 2 h followed by rise to -40°C for the period of 30 min. After the freezing step, primary drying was performed at -35°C and 0.2 mbar for 21 h, with consequent isobaric increase in temperature of 5°C per hour to 35°C, where the samples were kept for 2 h. After equilibration to 25°C, dry N<sub>2</sub> gas was used to obtain ambient pressure in the chamber. Before opening the chamber shelves, compression was utilized to close the vials. Aluminium crowns were placed on top of the rubbery stoppers to assure the stoppers location on the vial after the lyophilisation procedure. Visual observation revealed no collapses in the samples structure during freeze-drying. A few samples got a fissure in the middle of the cake, these vials were expelled from the analysis.

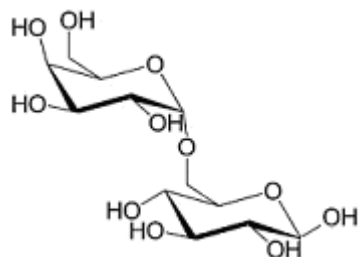
Trehalose



Cellobiose



Melibiose



Sucrose

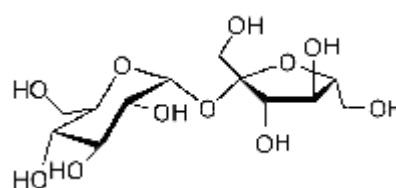


Figure 11. The molecular structure of disaccharides, studied in the present work.

The glass transition temperatures ( $T_g$ ) of the amorphous solids were evaluated using differential scanning calorimeter DSC823e (Mettler-Toledo Inc., Switzerland), which was equipped with multi-frequency modulated technique TOPEM. Samples were hermetically sealed in aluminium pans inside a glove box at relative humidity of about 5%. Generally almost the whole content of one vial was used to pack one aluminium pan (i.e. sample size



was 5-10mg). The  $T_g$  was evaluated by heating the samples at scanning rates of 2°C/min, 5°C/min, 10°C/min and 20°C/min to at least 20°C over their  $T_g$  under 50 ml/min dry N<sub>2</sub> flow.  $T_g$  was estimated using bisector method ( $T_g$  is the temperature at which the bisector of the angle between the two tangents intersecting the DSC curve). In TOPEM mode, it is necessary to specify some experimental parameters: the underlying scanning rate used was 2K/min, the amplitude of the temperature pulse +/- 0,5K, a switching time range of 15 to 30 s (the default values).

#### Heat capacity measurements

The heat capacity measurements of the amorphous and crystalline forms of the disaccharides were performed using ASTM method (E1269-05). The standard method covers specific heat capacity determination by differential scanning calorimetry. Terminology, methodology and practical advice can be found in the paper. The heat flow calibrations using sapphire standard was performed on daily bases, prior to specific heat capacity determination. The heat capacity measurements for all samples were performed using temperature program from 50°C below  $T_g$  to at least 20°C above  $T_g$ , with holding at the starting temperature for 4 min before initiation of the temperature program. Three runs in a row of the same sample were performed to assure consistent results. The heat capacity values used in the study represent average of minimum three samples.

#### $T_g$ dependence on scanning rate

Glass transition temperature dependence on the scanning rate was determined on the basis of the method developed by Moynihan et al [1974]. It was found that  $T_g$  value is dependent on heating or cooling rate, where faster scanning rates reveal higher values of  $T_g$ .  $T_g$  was estimated from the second heating run. The first heating run's purpose was to eliminate possible impact of thermal history of the sample. After the first run the sample was kept at temperature 15K above  $T_g$  with subsequent cooling at the same rate to 25°C. 4 minutes equilibration period was used between the first and the second heating. The  $T_g$  values used in the study represent average of three samples at corresponding heating rates of 2K/min, 5K/min, 10K/min and 20K/min.

Due to time limitations fragility data for trehalose and sucrose was not estimated using the method described above. The values of glass transition temperature dependence on heating rate for trehalose and sucrose was found in literature (Hancock et al. 1998). In their study lyophilized samples were analysed by means of a Seiko DSC (RDC-220). Their temperature program covered a region of at least 20K above  $T_g$  to at least 50K below  $T_g$  and included a preliminary heating run to remove possible thermal history. Heating rates employed were 5, 7, 10, 14, 20 and 30K/min. The activation energies for molecular motions were calculated from the slope of Arrhenius-type plots, which is the way used in the present study. The values of activation energies for sucrose (239kJ/mol) and trehalose (460kJ/mol) were used in the present study.

## 8. RESULTS AND DISCUSSION

### 8.1 The heat capacity measurements and $\gamma$ - parameter

The  $T_g$  values and fragility parameters of the four disaccharides are resumed in Table 3. The  $\gamma$ -parameter was calculated from heat capacity measurements of crystalline and amorphous forms, using Eq. 8. The heat capacity measurement of crystalline forms resulted in  $C_p$  curves versus temperature, the average trend line of which had excellent correlation coefficient of more than  $R^2=0.98$  and mean standard deviation of separate runs was 2.16% for melibiose, 5.87% for cellobiose, 9.53% for trehalose and 3.95% for sucrose (see an example on Figure 13). It should be mentioned that measurements on trehalose crystalline form have been accompanied with a degree of uncertainty, while several attempts to obtain anhydrous crystalline form using elevated temperatures and reduced pressure oven resulted in the sample amorphization. Despite numerous attempts to obtain anhydrous form of trehalose, a persistent endothermic peak at 90-100°C was observed, which was consistent with Sussich and co-workers (Sussich et al 1998) study results, where according to the microscope observations at 20 K min<sup>-1</sup>, trehalose dihydrate crystals were found to be stable to the dehydration even above 95 °C. These authors also reported total of 9.52% of the weight loss in the range around 100 degrees C at 1 K min<sup>-1</sup> using thermogravimetric experiments, corresponding to the loss of two water molecules caged in the hydrated structure.

According to research of Reisener (Reisener et al. 1962), anhydrous forms of trehalose can be prepared by keeping the dihydrate sample under vacuum at 85 °C for 4 h (alpha-polymorph) and at 130 °C for 4 h (for beta-polymorph). The dehydration conditions to obtain anhydrous form of trehalose used in the study are given in Table 4.

Table 3. Calorimetrically estimated values of  $T_g$  and fragility parameters for the four amorphous disaccharides.

disaccharide	$T_g$ [C]	$T_g$ [K]	m	D	$T_0$ [K]	$\gamma$	$\tau$ ( $T_g$ -50°C), days
Trehalose	117.8	391.0	61	12.97	289.2	0.728	43
Sucrose	71.6	344.8	36	29.18	192.4	0.794	4
Melibiose	94.8	367.9	78	9.54	292.2	0.813	64
Cellobiose	106.8	380.0	55	15.15	269.3	0.655	109

Table 4. Temperature and pressure parameters for trehalose dihydrate drying used in present study.

T [C]	pressure	t [h]	result
100	100mbar	0,5	Endotherm peak at 90-100°C. Hydrated form undisturbed.
100	100mbar	1	Absence of endotherm peak; melting enthalpy peak is of the same size and the same position, as dihydrate form.
110	100mbar	0.3	Amorphous form is obtained.
120	1 atm	0.83	Amorphous form is obtained.
80	100mbar	20	Amorphous form is obtained
50	100mbar	22	Endotherm peak at 90-100°C. Hydrated form undisturbed.
60	100mbar	2	Endotherm peak at 90-100°C. Hydrated form undisturbed.
60	100mbar	22	Endotherm peak at 90-100°C. Hydrated form undisturbed.

For calculation in the study, dihydrate form was used to obtain heat capacity values of crystalline form of trehalose.

The heat capacity measurement of amorphous forms resulted in  $C_p$  curves versus temperature, average trend line of which well before the glass transition were used to estimate the value of  $C_p$  at  $T_g$ , as illustrated in Figure 13. Good correlation coefficient of more than  $R^2=0.98$  is obtained for the average trend line and mean standard deviation of separate runs was 4.24% for melibiose, 4.94% for cellobiose, 3.76% for trehalose and 8.73% for sucrose. The mean

standard deviation values in measurements of amorphous forms are somewhat bigger than those of crystalline form. This can be attributed to overall sensitivity of DSC instrumentation.

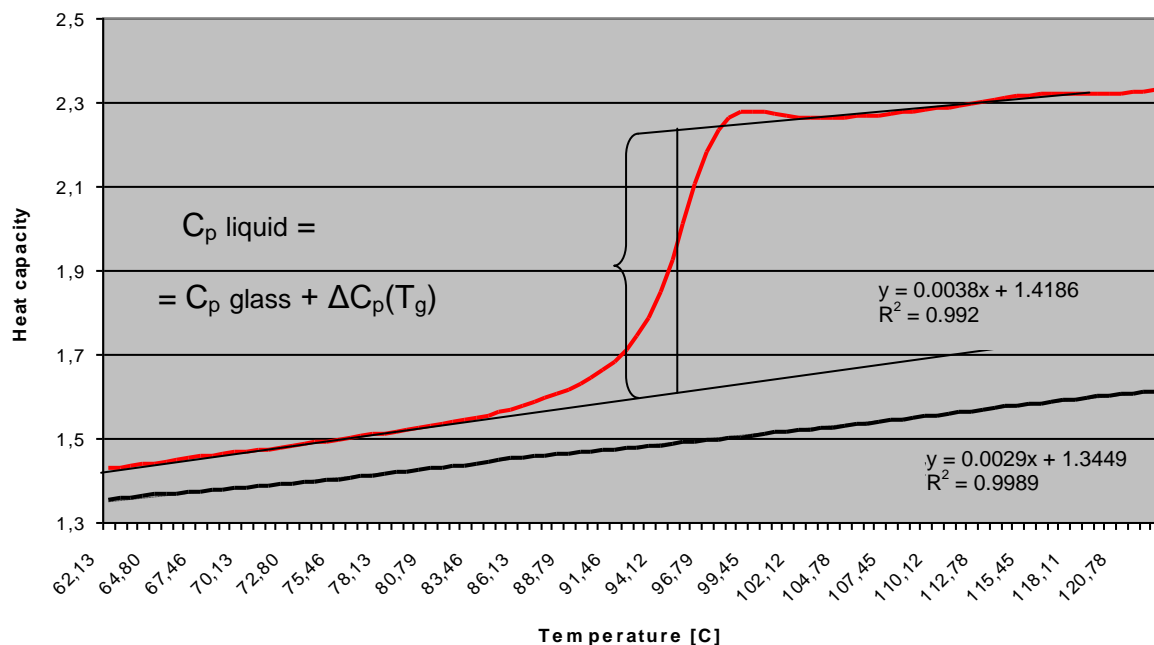


Figure 13. Heat capacities of crystalline (black) and amorphous (red) melibiose, measured by DSC. For the purpose of estimation of heat capacity value of amorphous form at  $T_g$ , linear extrapolation was used ( $y = 0.0038x + 1.4186$ ). Heat capacity value of supercooled liquid form at  $T_g$  is calculated by adding experimental mean  $\Delta C_p$  value.  $T_g$  value was estimated using bisector method (not shown on the curve).

The heat capacity values of supercooled liquids at  $T_g$  were calculated by adding mean  $\Delta C_p$  values, obtained from the experiment to the  $C_p(T_g)$  of amorphous form. An example of heat capacity value calculations is given in Table 5.

Table 5. Heat capacity value calculations for mellibiose. The equations are the linear trends of experimental heat capacity curves.  $T_g$  value of mellibiose (94.78°C equals 367.93K) was estimated using software of DSC.

form	$C_p$ equation	$C_p(T_g)$ value, J/(gK)
supercooled liquid	$C_p = C_p(\text{glass}) + \Delta C_p$	2.47
amorphous	$y = 0.0038x + 1.4186$	1.78
crystalline	$y = 0.0029x + 1.3449$	1.62

For comparison, literature values of  $\gamma$ -parameter were found for trehalose (0.80) and sucrose (0.76) (Shamblin et al. 1999). These literature values differ from estimated in the present study by 9% for trehalose and by 4.3% for sucrose.

The  $\gamma$ -parameter reflects relative differences between the heat capacities of the crystal, glass, and equilibrium liquid. The value of  $\gamma$ -parameter varies within interval of  $0 < \gamma < 1$ , Eq. 8. In case of  $\gamma \sim 1$ ,  $T_f$  does not diverge from  $T_g$  a lot (see Eq. 7) and the structure of the glass is not sensitive to changes in temperature. This is characteristic for strong behaviour. At the other extreme,  $\gamma = 0$ ,  $T_f = T$ , the molecular mobility of the glass is the same as in equilibrium liquid. In this case the original form of the VTF equation is valid below  $T_g$ , which corresponds to fragile behaviour. In fragile material only little resistance against structural degradation is observed with change in temperature. Therefore, the  $\gamma$ -parameter can serve an estimate for fragility of the glass, where  $\gamma = 1$  corresponds to a “strong” glass (with thermally activated or Arrhenius behaviour of relaxation process) and  $\gamma = 0$  corresponds to a “fragile” glass (or VTF behaviour below  $T_g$  and correspondingly the largest deviations from the Arrhenius law).

According to  $\gamma$ -parameter ranking melibiose appears to be the strongest compound under the study (see Table 3). The result is not in agreement with the fragility ranking based on the regular approach described below. The disagreement in the ranking can be attributed to the sensitivity of the  $\gamma$ -parameter to heat capacity measurements. The value of  $\gamma$ -parameter contains the mean standard deviation, the marginal of which is comparable with the differences between  $\gamma$ -parameters of the compounds under the study. The  $\gamma$ -parameter for the disaccharides evaluated by means of the thermal technique can be used only to identify the compounds to be fragile (all the compounds are fragile). The comparison between the disaccharides according to the parameter is not reliable due to the mean standard deviation related to the estimation.

## 8.2 Fragility

Fragility has been used as a helpful mean for classifying amorphous materials. The results of the present study are not quite consistent with steepness index data from literature. For example, Duddu et al (Duddu et al. 1997) reported based on enthalpy recovery experiments  $m$  values of 100 and 125 for trehalose and sucrose respectively. Gusseme et al. (Gusseme et al. 2003) reported  $m$  value for trehalose of 107. Other researchers (Sussich et al. 2001) evaluated

steepness index of trehalose,  $m$ , to be 160–180. Dranca and co-workers (Dranca et al. 2009) determined  $m = 77$  for trehalose, and  $m = 88$  for sucrose.

Fragility data for the four disaccharides studied in the present work is presented in Table 3. All the compounds can be classified as fragile; with strength parameter  $D < 30$  values generally representing fragile materials (Crowley and Zografi 2001).  $D$  values found in literature for trehalose and sucrose were 5.1 and 7.3 respectively (Shamblin et al. 1999). Another research estimated  $D$  values for trehalose and sucrose to be 6.988 and 8.57 respectively (Hatley 1997). The fragility values calculated in the present study reveal the same trend, i.e. trehalose being more fragile, as compared to sucrose, but the values data diverge from those found in literature significantly.

Stepwise determination of melibiose fragility is presented in Table 6 and Figure 14.

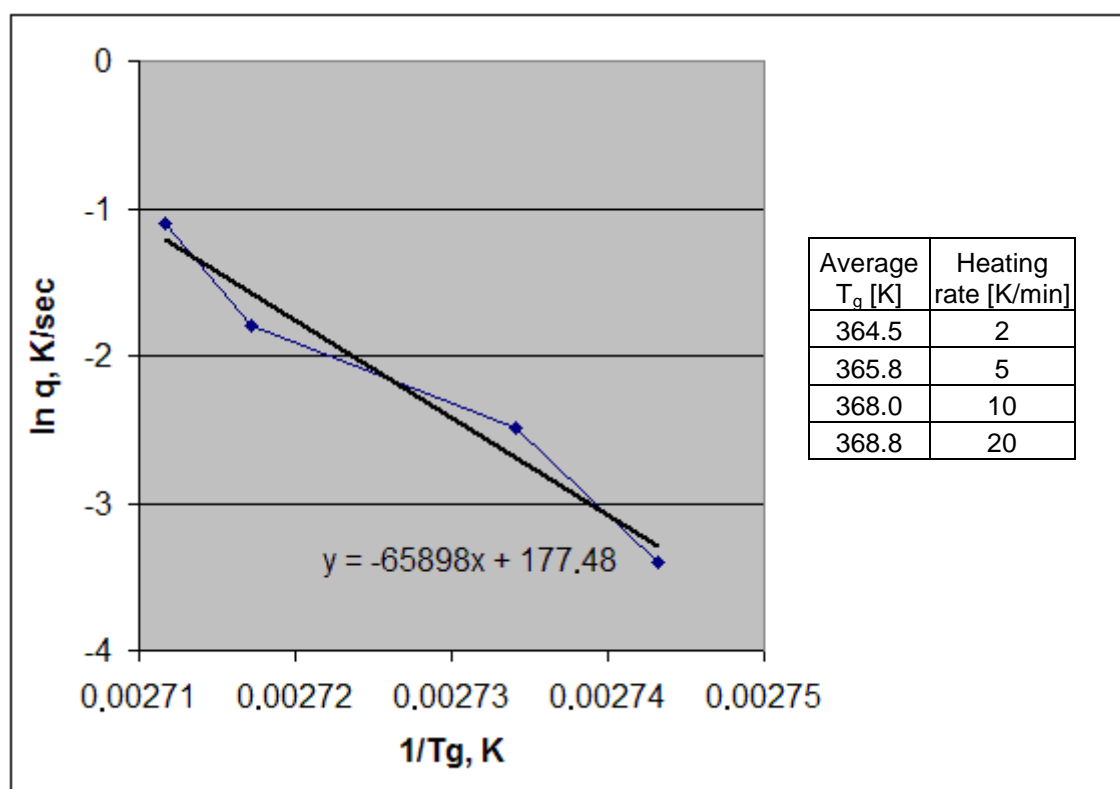


Figure 14.  $T_g$  dependence on scanning rate for melibiose.

A visualization of general interrelation between the two terms of fragility (strength parameter  $D$  and steepness index  $m$ ) is given in Figure 15. Fragile material is characterized by a small value of  $D$  and a big value of  $m$ , while strong material is characterized by a big value  $D$  and a small value  $m$ .

Table 6. Stepwise determination of melibiose fragility values, as estimated in the present study.

Step 1	The slope of the curve $\ln q$ vs $1/T_g$	65898
Step 2	$\Delta H(T_g) = 8,314 \times (65898) =$	547876
Step 3	$m = \Delta H(T_g) / (2,303 \times 8,314 \times T_g) =$	77,77
Step 4	$D = (2,303 \times m_{\min}^2) / (m - m_{\min}) =$	10
Step 5	$T_0 = T_g \times (1 - m_{\min}/m)$	292

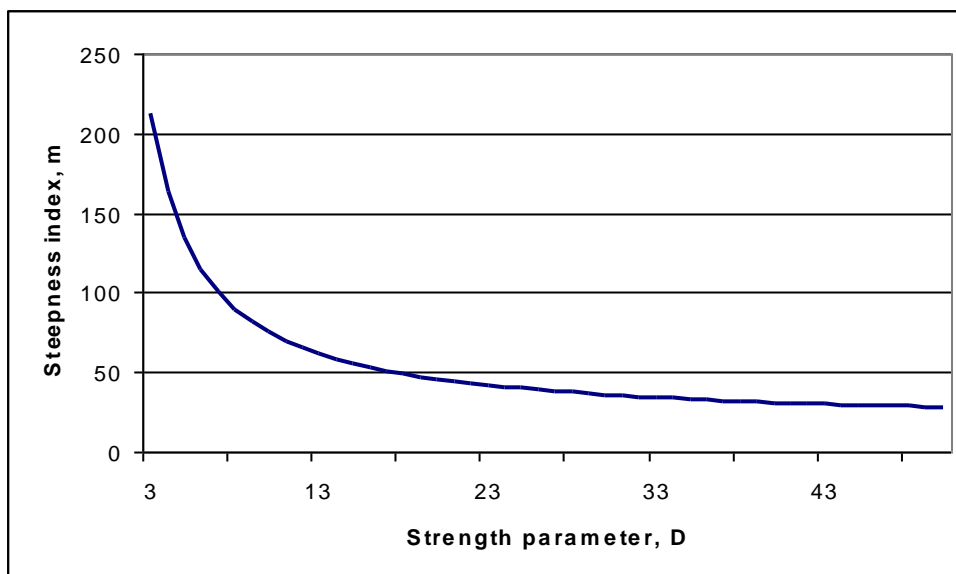


Figure 15. A visualization of the interrelation between strength parameter D and steepness index m.

The measurements for evaluation of fragility parameters require careful instrumental calibration and experimental conditions control. The parameters for fragility quantification cannot be evaluated directly, but require a number of intermediate calculations, which creates potential for mistakes. That could be the reason for the scattering of fragility values reported in the literature for the same material. Mostly it has been reported that careful precautions had been taken to prevent moisture uptake into the samples. And the observed differences in fragility data can not be attributed to different moisture residuals alone. However, it has been recognized that different methods of preparation of amorphous material result in different thermodynamic properties for the same substance, what could be reflected in fragility values. The observed variations are even more significant, when different experimental techniques are employed and different estimation methods are used, although different estimation methods are not expected to reveal different values of fragility, since it is an intrinsic property of each material (Wang et al. 2002).

### 8.3 The initial relaxation time

The initial relaxation time dependence on storage temperature is presented in Figure 16. At  $T_g$ , all materials have the same value of relaxation time (100 s). However, when the temperature is reduced, the relaxation times of the disaccharides do not shear similar changes. Comparing the values at temperature  $T_g-50$ , often recommended to be the guiding line for storage condition choice, significant differences can be observed.

For comparison purpose relaxation times for trehalose and sucrose were found in literature. The results of two studies and the values from the present study are shown in Table 7. The measurements in both reference articles were performed using isothermal microcalorimetry, where enthalpy recovery was monitored for a few day's time (70h and 90h). The relaxation times of lyophilized samples in both studies were estimated using a derivative equation of the modified stretched exponential (MSE) function in addition to the KWW equation.

Table 7. Relaxation time (s), found in literature and calculated in the present study. Ref. A: Liu et al. 2002. Ref.B: Shamblin et al. 2006.

	ref.A		ref.B		The present study	
Temp., °C	Trehalose	Sucrose	Trehalose	Sucrose	Trehalose	Sucrose
40	121 320	32 796	284 400	50 760	3 088 238 400	9 068
50	60 840	11 160	93 240	11 880	59 519 792	1 813
60			47 880	5 400	3 694 595	406

The purpose of the present study was to provide an estimate for relaxation time at low temperatures (as compared to  $T_g$ ). From these considerations the data for sucrose is not expected to be close to other experiments results, since 50°C is only about 20 degrees below anhydrous sucrose  $T_g$ . As for trehalose, a huge difference in estimation by means of mentioned techniques is observed. The results from literature on isothermal microcalorimetry measurements suggest that for amorphous trehalose relaxation time at  $T=50^\circ\text{C}$  is about 1 day (93 240sec), while the results of the present study state the time to be 688days or 1.8 years.

The difference in the results for trehalose (see Table 7, literature values versus this study) could be attributed to the differences in the methods of evaluation. Isothermal microcalorimetry allows to monitor directly the changes in enthalpy of the sample. However,



the equation used to determine the relaxation time was the KWW- based. The approach has been criticized for an unreliable estimation of relaxation process on longer time scales, since there is no reliable method to extrapolate the results of few days enthalpy relaxation experiment to the timescale of a few years. Another factor that could have an influence on the results of isothermal microcalorimetry is that the samples were analyzed without procedures, which could erase thermal history of the samples. Still another potential for mistakes could arise from the fact, that not all the required parameters were evaluated from the experimental measurements, but a part was reported to be obtained from literature.

Shamblin and co-workers (Shamblin et al. 1999) evaluated mean relaxation times of freshly quenched glasses using similar approach. Their results reveal mean relaxation time for sucrose of 3 years at temperature  $T=60^{\circ}\text{C}$  and trehalose at  $T=100^{\circ}\text{C}$ , based on estimation of unaged glass.

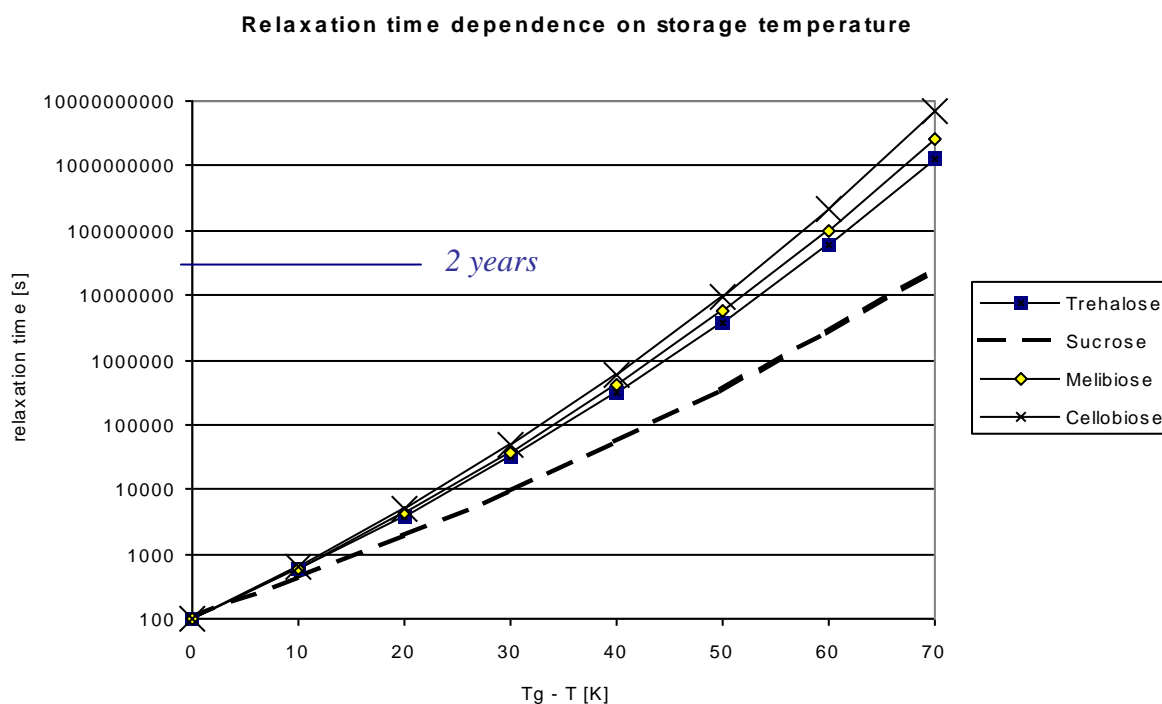


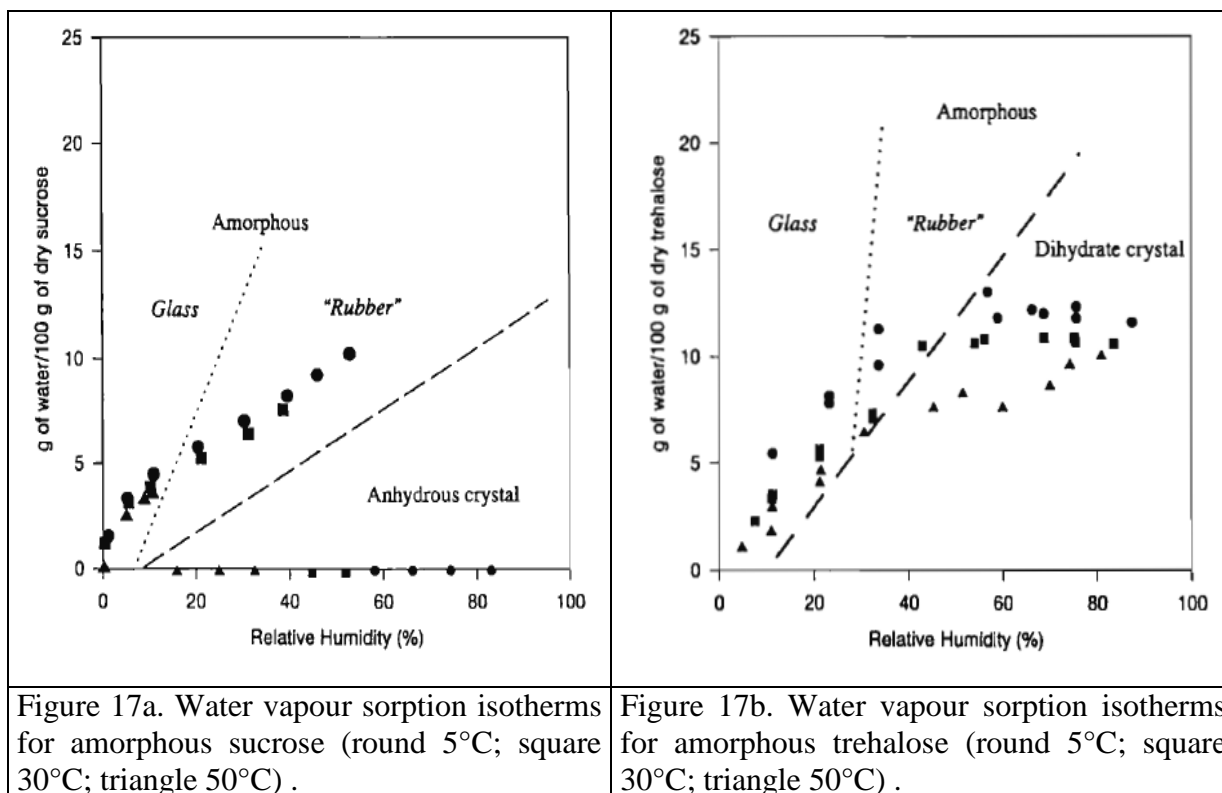
Figure 16. Initial relaxation times of amorphous disaccharides as the function of  $T_g - T$ . The blue line corresponds to 2 years' time = 63 072 000s.

The results of the study can be interpreted so that sucrose should have the greatest tendency toward crystallization than other three disaccharides. Similar conclusion can be made on  $T_g$  values alone, since sucrose has the lowest  $T_g$  of the four disaccharides.

Trehalose has got much attention in studying glassy state dynamics. One of the reason for that is its exceptional high  $T_g$  value, the highest among disaccharides (Roos and Karel 1991b), which is reflected in the dynamics of trehalose-water systems, which becomes amorphous at severe desiccation conditions.

#### 8.4 Other stability considerations for formulation with amorphous content

A glass exposure to water vapours can result in amorphous structure collapse and crystallization. Timing, temperature and RH conditions for the process may vary. Hancock and Dalton (Hancock and Dalton 1999) studied moisture sorption of amorphous trehalose and sucrose at different temperatures. The results of their study can be resumed in Figure 17a and 17b.



The results of their study revealed no general trend for the critical humidity-temperature conditions required for crystallization of the amorphous sugars, but it is easy to observe that, at high temperature, sucrose crystallization tendency is markedly higher than that of trehalose. When temperature is reduced to 5°C, both disaccharides would experience crystallization at about 55% RH.

Therefore, the foregoing discussion on the disaccharides tendency to crystallize from amorphous state due to temperature and RH conditions underlines the same trend of stability, which can be derived from  $T_g$  difference alone (the higher  $T_g$  means the more stable amorphous system).

It is generally accepted that excipients in lyophilized formulation should remain amorphous in order to provide stabilizing effect. Crystallization of excipients results in changes in molecular interactions, where the stabilization of labile substance (i.e. protein) can be questioned. Significant mobility can be observed when amorphous material is stored above its  $T_g$ . Then collapse of amorphous structure is possible on the time scale of single observation. However, knowledge of the formulation  $T_g$  is not enough to validate the optimal storage conditions.

$T_g'$  of formulation is dependent on water content. Water is an ambient substance, which is readily sorbed into amorphous solids. When some water is sorbed, the  $T_g'$  of the formulation is reduced and can exceed the chosen storage temperature. Therefore, humidity considerations need to be taken into account.

Different materials demonstrate different molecular mobility in the amorphous state. Molecular mobility of any glass is temperature dependent. Basically, the lower the temperature, the slower the molecular motions. However, the only certain guide for the temperature choice is  $T_0$ , where the molecular mobility is considered to cease. More fragile materials demonstrate higher  $T_0$  values, and therefore they can be considered more stable during storage (providing that the materials share similar  $T_g$  values).

## 9. CONCLUSIONS

In the present study a calorimetric method to evaluate molecular mobility of structurally related amorphous disaccharides was estimated. The purpose of the study was to obtain initial relaxation time, which could be used as an estimate of average relaxation times at low temperatures. The average relaxation time increases when temperature is reduced. At significantly low temperatures (as compared to  $T_g$ ) molecular motions are slow enough to be considered negligible as compared to the pharmaceutically relevant periods of time, and the initial relaxation time parameter could serve an estimate of average relaxation time.

Molecular mobility was found to be of similar magnitude in cellobiose, trehalose and melibiose. Sucrose was found to exhibit greater molecular mobility and therefore require lower storage temperatures (as compared to  $T_g$ ), than the other disaccharides.

Some of the data, obtained from the present study, is not in agreement with values found in literature. The results, obtained with the method of the present study, are very dependent on the slope in plotting  $\ln q$  vs.  $1/T_g$ , and even small fluctuations in the estimation can lead to different fragility values and consequently to different relaxation times.  $T_g$  value alone is dependent on many factors, such as moisture content of the material, method of amorphous solid preparation, thermal history of the sample, instrumentation choice as well as the heating rate and the method for obtaining  $T_g$  from DSC thermogram, while using calorimetry. The variation in the results can be attributed as well to the overall dependence of estimation of glass transition on the adjustable variables used in modulated DSC.

The conclusions suggest that the method used in the present study is quite difficult to apply without supportive information from other techniques. However, the final results reveal values for relaxation times well below  $T_g$ , which are in reasonable agreement with modern theoretical understanding of glassy state dynamics. The molecular mobility in amorphous material is expected to be significant in the temperature range up to  $T_g-50^\circ\text{C}$  (Hancock et al. 1995) and storage temperature of  $T_g-50^\circ\text{C}$  is expected to be a guideline for pharmaceutically relevant timescale. This is consistent with the results of the present study, where 2 years relaxation time was estimated for three of the four disaccharides (cellobiose, trehalose and melibiose) at temperature of  $T_g-55^\circ\text{C}$ .

## 10 REFERENCES

- Allison SD, Dong A, Carpenter JF: Counteracting effects of thiocyanate and sucrose on chymotrypsinogen secondary structure and aggregation during freezing, drying, and rehydration. *Biophys J* 71: 2022–2032, 1996
- Angell CA: Formation of glasses from liquids and biopolymers. *Science* 267: 1924-1935, 1995
- Biliaderis CG, Page CM, Maurice TJ, and Juliano B: Thermal characterization of rice starches: A polymeric approach to phase transitions of granulars. *J Agr Food Chem* 34: 6-14, 1986
- Böhmer R, Ngai KL, Angel CA, Plazek DJ: Nonexponential relaxations in strong and fragile glass formers. *J Chem Phys* 99 (5): 4210-4209, 1993
- Briggner LE, Buckton G, Bystrom K, Darcy P: The use of isothermal microcalorimetry in the study of changes in crystallinity induced during the processing of powders. *Int. J. Pharm.* 105: 125–135, 1994
- Broadhead J, Edmond SKR, Rhodes CT: The spray drying of pharmaceuticals. *Drug Dev Ind Pharm* 18:1169–1206, 1992
- Brummer B, Swick P, Link M, Hart: In-situ lyophilisation of vaginal suppository in unit dose applicator and resultant product 1997. US Patent 5,656,283
- Bystrom K and Briggner L: Microcalorimetry - a novel technique for characterization of powders. *Drug Deliv IV*: 297-302, 1994
- Carpenter JF, Pikal MJ, Chang BS, Randolph TW: Rational design of stable lyophilized protein formulations: Some practical advice. *Pharm Res* 14: 969–975, 1997
- Chang S, Horman JA, Bestul AB: Heat capacities and related thermal data for diethyl phthalate crystal, glass, and liquid to 360°K. *J Res Nat Bur Stand* 71(4): 293-305, 1967
- Chang BS, Beauvais RM, Dong A, Carpenter JF: Physical factors affecting the storage stability of freeze-dried interleukin- 1 receptor antagonist: Glass transition and protein conformation, *Arch Biochem Biophys* 331: 249-258, 1996
- Chang L, Shepherd D, Sun J, Ouellette D, Grant KL, Tang X(C), Pikal MJ: Mechanism of Protein Stabilization by Sugars During Freeze-Drying and Storage: Native Structure Preservation, Specific Interaction, and/or Immobilization in a Glassy Matrix? *J Pharm Sci* 94, 7: 1427-1444, 2005
- Chen X, Bates S, Morris KR: Quantifying amorphous content of lactose using parallel beam X-ray powder diffraction and whole pattern fitting. *J Pharm Biomed Anal* 26: 63–72, 2001
- Constantino HR, Carrasquillo KG, Cordero RA, Mumenthaler M, Hsu CC, Greibenow K: Effect of excipients on the stability and structure of lyophilized recombinant human growth hormone, *J Pharm Sci* 87,11: 1412- 1420, 1998

- Corveleyn S, Remon JP: Formulation and production of rapidly disintegrating tablets by lyophilisation using hydrochlorothiazide as a model drug. *Int J Pharm* 152: 215–225, 1997
- Corveleyn S, Remon JP: Formulation of a lyophilised dry emulsion tablet for the delivery of poorly soluble drugs. *Int. J. Pharm* 166: 65–74, 1998
- Cowie JMG, Harris S, McEwen IJ: Physical aging in poly(vinyl acetate). 2. Relative rates of volume and enthalpy relaxation. *Macromolecules* 31: 2611–2615, 1998
- Craig DQM: Applications of low frequency dielectric spectroscopy to the pharmaceutical science. *Drug Dev Ind Pharm* 18: 1207–1223, 1992
- Crowe JH, Carpenter JF, Crowe LM: The role of vitrification in anhydrobiosis. *Annu Rev Physiol* 60: 73, 1998
- Crowley KJ, Zografi G: The use of thermal methods for predicting glass-former fragility. *Thermochim Acta* 380: 79–93, 2001
- Dranca I, Bhattacharya S, Vyazovkin S, Suryanarayanan R: Implications of global and local mobility in amorphous sucrose and trehalose as determined by differential scanning calorimetry. *Pharm Res* 26, 5: 2009
- Duddu SP, Sokolski TD: Dielectric analysis in the characterization of amorphous pharmaceutical solids. 1. Molecular mobility in poly(vinylpyrrolidone)-water systems in the glassy state. *J Pharm Sci* 84(6):773–6, 1995
- Ediger MD, Angell CA, Nagel SR: Supercooled liquids and glasses. *J Phys Chem* 100: 13200–13212, 1996
- Elamin AA, Sebhatu T, Ahlneck C: The use of amorphous model substances to study mechanical activated materials in the solid state. *Int J Pharm* 119: 25–36, 1995
- Goldstein: Viscous liquids and the glass transition: a potential energy barrier picture. *J Chem Phys* 51: 3728–3739, 1969
- Gusseme A, Carpentier L, Willart JF, Descamps M: Molecular mobility in supercooled trehalose, *J Phys Chem B* 107: 10879–10886, 2003
- Hancock BC, Dalton CR: The effect of temperature on water vapor sorption by some amorphous pharmaceutical sugars. *Pharm Dev Technol* 4(1): 125–131, 1999
- Hancock BC, Zografi G: Characteristics and significance of the amorphous state in pharmaceutical systems. *J Pharm Sci* 86: 1–12, 1997
- Hancock BC, Shamblin SL, Zografi G: Molecular mobility of amorphous pharmaceutical solids below their glasstransition temperatures. *Pharm Res* 12: 799–806, 1995
- Hancock BC, Dalton CR, Pikal MJ, Shamblin SL: A pragmatic test of a simple calorimetric method for determining the fragility of some amorphous pharmaceutical materials. *Pharm Res* 15, 5: 762–767, 1998

- Hatley RHM: Glass Fragility and the Stability of Pharmaceutical Preparations-Excipient Selection. *Pharm Dev Technol* 2(3): 257-264, 1997
- Hill VL, Graig DQM, FeelyLC: The effects of experimental parameters and calibration on MTDSC data. *Int J Pharm* 192: 21–32, 1999
- Hodge IM: Strong and fragile liquids - a brief critique. *J Non-Cryst Solids* 202: 164- 172, 1996
- Hogan SE and Buckton G: The application of Near Infrared Spectroscopy and dynamic vapor sorption to quantify low amorphous contents of crystalline lactose. *Pharm Res* 18: 112–116, 2001
- Hsu C, Nguyen H, Yeung D, Brooks D, Koe G, Bewley T, Pearlman R: Surface denaturation at solid void interface - A possible pathway by which opalescent particulates form during the storage of lyophilized tissue-type plasminogenactivator at high-temperatures. *Pharm Res* 12(1): 69-77, 1995
- Johari GP, Goldstein M: Viscous liquids and the glass transition. II. Secondary relaxations. *J Chem Phys* 53: 2372- 2388, 1970
- Johari GP: Intrinsic mobility of molecular glasses. *J Chem Phys* 58: 1766–1770, 1973
- Jouppila K, Roos YH: Glass transitions and crystallization in milk powders. *J Dairy Sci* 77: 2907–2915, 1994
- Kalichevsky MT, Jaroszkiewicz EM, Ablett S, Blanshard JMV, Lillford PJ: The glass transition of amylopectin measured by DSC, DMTA and NMR. *Carbohydr Polym* 18, 77-88, 1992
- Kamat MS, Lodder RA, DeLuca PP: Near-infrared spectroscopic determination of residual moisture in lyophilized sucrose through intact glass vials. *Pharm Res* 6: 961–965, 1989
- Kim SS, Kim SJ, Moon YD, Lee YM: Thermal characteristics of chitin and hydroxypropyl chitin. *Polymer* 35 (15): 3212–3216, 1994
- Law D, Krill SL, Schmitt EA, Fort JJ, Qiu Y, Wang W, Porter WR: Physicochemical considerations in the preparation of amorphous ritonavir(ethylene glycol) 8000 solid dispersions. *J Pharm Sci* 90: 1015–1025, 2001
- Liao YY, Brown MB, Quader A, Martin GP: Protective mechanism of stabilizing excipients against dehydration in the freeze-drying of proteins, *Pharm Res* 19,12: 1854-1861, 2002]
- Lindsey CP, Patterson GD: Detailed comparison of the Williams-Watts and Cole-Davidson functions. *J Chem Phys* 73: 3348–3357, 1980
- Liu J, Physical characterization of pharmaceutical formulations in frozen and freeze-dried solid states: techniques and applications in freeze-drying development. *Pharm Dev Technol* 11: 3–28, 2006

- Liu J, Rigsbee DR, Stotz C, Pikal MJ: Dynamics of pharmaceutical amorphous solids: the study of enthalpy relaxation by isothermal microcalorimetry. *J Pharm Sci* 91: 1853-1862, 2002
- Marsac PJ, Konno H, Taylor LS: A comparison of the physical stability of amorphous felodipine and nifedipine systems. *Pharm Res* 23,10: 2306-2316, 2006
- Mazzobre MF, Longinotti MP, Corti HR, Buera MP: Effect of salts on the properties of aqueous sugar systems, in relation to biomaterial stabilization. 1. Water sorption behavior and ice crystallization/melting, *Cryobiology* 43: 199–210, 2001
- Moynihan CT, Eastal AJ, Wilder J, Tucker J: Dependence of the glass transition temperature on heating and cooling rate. *J Phys Chem* 78 (26): 2673–2677, 1974
- Moynihan CT: Structural relaxation and the glass transition. *Rev. Mineral.* 32: 1–19, 1995
- Noel TR, Parker R, Ring SG: Effect of molecular structure and water content on the dielectric relaxation behaviour of amorphous low molecular weight carbohydrates above and below their glass transition. *Carb Res* 329: 839–845, 2000
- Overcashier DE, Patapoff TW, Hsu CC: Lyophilization of protein formulations in vials: Investigation of the relationship between resistance to vapor flow during primary drying and small-scale product collapse. *J Pharm Sci* 88: 688–695, 1999
- Pereswetoff-Morath L and Edman P: Dextran microspheres as potential nasal drug delivery system for insulin - in vitro and in vivo properties. *Int J Pharm* 124: 37-44, 1995
- Reisener HJ, Goldschmid HR, Ledingham GA, Perlin AS: Formation of trehalose and polyols by wheat stem rust (*Puccinia graminis tritici*) uredospores. *Can J Biochem Physiol* 10: 1248-1251, 1962
- Pikal MJ, Roy ML, Shah S. Mass and heat transfer in vial freeze-drying of pharmaceuticals: role of the vial. *J. Pharm. Sci.* 73: 1224–1237, 1984
- Pikal MJ, Shah S, Senior D, Lang JE: Physical chemistry of freeze-drying: Measurement of sublimation rates for frozen aqueous solutions by a microbalance technique. *J Pharm Sci* 72(6): 635-650, 1983
- Pikal MJ: Freeze-drying of proteins. Part I: Process design. *BioPharm* 3(8): 18-27, 1990a
- Pikal MJ: Freeze-drying of proteins part II: formulation selection. *Bio Pharm* 3: 26–30, 1990b
- Rendell RW, Ngai NK, Plazek DJ: Volume dependent rate processes predicted by the coupling model. *J Non-Cryst Solids* 131–133: 942–948, 1991
- Roos Y, Karel M: Amorphous state and delayed ice formation in sucrose solutions. *Int J Food Sci Technol* 26: 553–566, 1991a
- Roos Y, Karel M: Water and molecular weight effects on glass transitions in amorphous carbohydrates and carbohydrate solutions. *J Food Sci* 56: 1676–1681, 1991b



Royall PG, Graig DQM, Doherty C: Characterization of the glass transition of an amorphous drug using modulated DSC. *Pharm Res* 15, 7: 1117-1121, 1998

Ruan RR, Long Z, Song A, Chen PL: Determination of the glass transition temperature of food polymers using low field NMR, *Lebensm-Wiss u-Technol* 31: 516-521, 1998

Saleki-Gerhardt A, Ahlneck C, Zografi G: Assessment of disorder in crystalline solids. *Int J Pharm* 101: 237-247, 1994

Saleki-Gerhardt A, Stowell JG, Byrn SR, Zografi G: Hydration and dehydration of crystalline and amorphous forms of raffinose. *J Pharm Sci* 84: 318–323, 1995

Shamblin SL, Tang X, Chang L, Hancock BC, Pikal MJ: Characterization of the time scales of molecular motion in pharmaceutically important glasses. *J Phys Chem B* 103: 4113-4121, 1999

Shamblin SL, Hancock BC, Pikal MJ: Coupling between chemical reactivity and structural relaxation in pharmaceutical glasses. *Pharm Res* 23,10: 2254-2268, 2006

Searles JA, Carpenter JF, Randolph TW: The ice nucleation temperature determines the primary drying rate of lyophilization for samples frozen on a temperature-controlled shelf. *J. Pharm. Sci.* 90: 860–871, 2001

Seyler RJ: Assignment of the glass transition, ASTM special technical publication, Stp, 1994

Sussich F, Urbani R, Princivale F, Cesa`ro A: Polymorphic amorphous and crystalline forms of trehalose. *J Am Chem Soc* 120: 7893-7899, 1998

Sussich F, Skopec C, Brady J, Cesa`ro A: Reversible dehydration of trehalose and anhydrobiosis: from solution state to an exotic crystal? *Carbohydr Res* 334:165–176, 2001

Tang X(C), Pikal MJ: Design of Freeze-Drying Processes for Pharmaceuticals: Practical Advice. *Pharm Res* 21,2: 191- 200, 2004

Tang X(C), Pikal MJ, Taylor LS, A spectroscopic investigation of hydrogen bond patterns in crystalline and amorphous phases in dihydropyridine calcium channel blockers. *Pharm Res* 19, 4: 477-483, 2002

Tsukushi I, Yamamuro O, Suga H: Heat capacities and glass transitions of ground amorphous solid and liquid-quenched glass of tri-*O*-methyl-[ $\alpha$ ]-cyclodextrin. *J Non-Cryst Solids* 175: 187–194, 1994

Voorhees PW: The Theory of Ostwald Ripening. *J Stat Phys* 38: 231-252, 1984

Wang W: Lyophilization and development of solid protein pharmaceuticals. *Int J Pharm* 203: 1–60, 2000

Wang LM, Velikov V, Angell CA: Direct determination of kinetic fragility indices of glassforming liquids by differential scanning calorimetry: kinetic versus thermodynamic fragilities. *J Chem Phys* 117: 10184–10192, 2002

Wang B, Tchessalov S, Cicerone MT, Warne NW, Pikal MJ: Impact of sucrose level on storage stability of proteins in freeze-dried solids: II. Correlation of aggregation rate with protein structure and molecular mobility. *J Pharm Sci* 98, 9: 3145-3166, 2009

Wolkers WF, Oldenhof H, Alberda M, Hoekstra FA: A Fourier transform infrared microspectroscopy study of sugar glasses: application to anhydrobiotic higher plant cells, *Biochim Biophys Acta* 1379: 83-96, 1998